
ECHOES OF BERT: DO MODERN LANGUAGE MODELS REDISCOVER THE CLASSICAL NLP PIPELINE?

Michael Li[✉] Nishant Subramani[✉]

[✉]Carnegie Mellon University - Language Technologies Institute
 {ml16, nishant2}@cs.cmu.edu

ABSTRACT

Large transformer-based language models dominate modern NLP, yet our understanding of how they encode linguistic information relies primarily on studies of early models like BERT and GPT-2. Building on prior BERTology work, we analyze 25 models spanning classical architectures (BERT, DeBERTa, GPT-2) to modern large language models (Pythia, OLMo-2, Gemma-2, Qwen2.5, Llama-3.1), probing layer-by-layer representations across eight linguistic tasks in English. Consistent with earlier findings, we find that hierarchical organization persists in modern models: early layers capture syntax, middle layers handle semantics and entity-level information, and later layers encode discourse phenomena. We dive deeper, conducting an in-depth multilingual analysis of two specific linguistic properties - lexical identity and inflectional morphology - that help disentangle form from meaning. We find that lexical information concentrates linearly in early layers but becomes increasingly nonlinear deeper in the network, while inflectional information remains linearly accessible throughout all layers. Additional analyses of attention mechanisms, steering vectors, and pretraining checkpoints reveal where this information resides within layers, how it can be functionally manipulated, and how representations evolve during pretraining. Taken together, our findings suggest that, even with substantial advances in LLM technologies, transformer models learn to organize linguistic information in similar ways, regardless of model architecture, size, or training regime, indicating that these properties are important for next token prediction. Our code is available at https://github.com/ml5885/model_internal_sleuthing

1 INTRODUCTION

Large transformer-based language models (LMs) are widely used for tasks such as text generation, question answering, and code completion (Workshop, 2023; Groeneveld et al., 2024; Llama, 2024; Hui et al., 2024) However, how these models internally represent linguistic information remains an active research area. Prior work suggests a hierarchical organization where different layers specialize in capturing distinct levels of linguistic structure, from surface features to syntax and semantics (Jawahar et al., 2019; Tenney et al., 2019a; Rogers et al., 2020).

But these studies focus only on first-generation LMs such as BERT and GPT-2 (Devlin et al., 2019; Radford et al., 2019). Since then, language technology has transformed dramatically - today's models are far larger, trained on much more data, and adapted through extensive post-training procedures (Brown et al., 2020; Groeneveld et al., 2024; Lambert et al., 2025). We ask: how do modern LMs encode linguistic structure, and how do these representations differ from those in earlier models? In particular, do modern LMs *rediscover the classical NLP pipeline* suggested by prior probing work (Tenney et al., 2019a)?

In addition to probing for these properties, we perform a focused case study on two linguistic properties: lexical identity and inflectional morphology. Consider the words *walk*, *walked*, *jump*, and *jumped*. Do language models group words by shared meaning (*walk*, *walked*) or by shared grammar (*walked*, *jumped*)? More broadly, where and how do LMs encode a word's lemma (its lexical identity) and its grammatical form (inflectional morphology)?

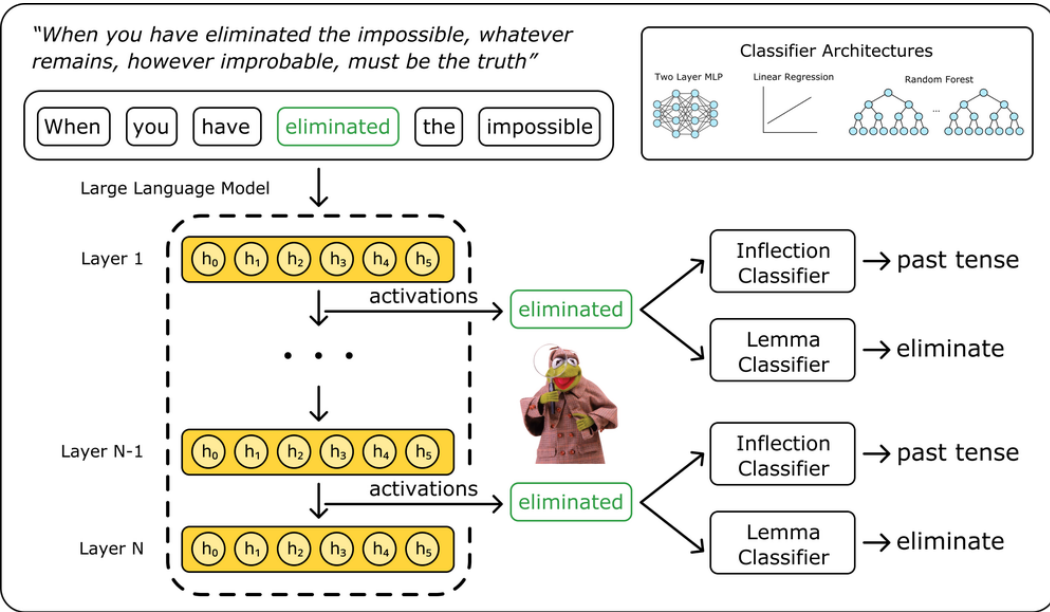


Figure 1: Overview of our classifier methodology. We extract hidden state activations from each model layer for target words and train classifiers for token, span and pairwise edge predictions (POS, dependencies, constituents, NER, SRL, SPR, coreference, and relations), as well as word-level lemma and inflection prediction. We compare linear regression, MLP, and random-forest classifiers, compute selectivity using control labels, and summarize where performance emerges with expected layer and center of gravity.

To answer these questions, we conduct probing experiments for each of these linguistic properties within model representations (hidden state activations). We train classifiers on 25 models spanning different architectures, sizes, and training regimes to determine if they process English linguistic structure in a hierarchical manner. For lexical identity and inflectional morphology, we dig deeper, examining six typologically diverse languages: English, Chinese, German, French, Russian, and Turkish. We also probe attention heads and pretraining checkpoints, find steering vectors, and analyze intrinsic dimensionality, to show where these two linguistic aspects live within layers, how they evolve during pretraining, and how they can be functionally manipulated. We find that:

1. Modern LMs consistently discover the classical NLP pipeline: early layers process surface and syntactic information, middle layers emphasize semantic and entity-level information, and later layers capture discourse.
2. Lexical information is predominantly encoded in early layers and becomes increasingly non-linear deeper in the network, while inflectional morphology remains linearly accessible across layers and languages.
3. Lexical identity and inflectional morphology representations emerge early in pretraining, and are robust across architectures, sizes, and languages. In particular, we find that inflectional features occupy compact, linearly accessible subspaces in the residual stream, enabling effective steering interventions.

2 BERTOLOGY: PROBE DESIGN AND METRICS

We study how language models encode linguistic information by training simple probabilistic classifiers on layer-wise residual-stream activations.¹ If a classifier recovers a property (e.g., POS, lemma) from a layer ℓ , we infer that the information is *encoded and accessible* at that layer; comparing layers shows how it evolves with depth.

¹We use representations, activations, and neurons interchangeably.

2.1 PROBE DESIGN

We follow the edge probing task design of Tenney et al. (2019b). For *token* tasks (e.g., POS), we use the representation of the last subword token for the target word. For *span* tasks (e.g., constituents, NER, SRL, SPR), we represent a span by mean-pooling its subword token representations. For *pair/edge* tasks (e.g., coreference, dependency arcs, relations), we encode a pair (s_1, s_2) as $[r_{s_1}; r_{s_2}; r_{s_1} \circ r_{s_2}; |r_{s_1} - r_{s_2}|]$, where r_s is the token or span representation, \circ is elementwise product, and $|\cdot|$ is absolute value.

We train linear regression and two-layer multi-layer perceptron (MLP) classifiers with cross-entropy loss on top of representations from each individual layer. Unlike Tenney et al. (2019a), who uses scalar mixing weights to fuse information across layers, we do not train probes on combinations of multiple layers. Our goal is analytical rather than predictive: we care about isolating where in the model each property becomes accessible, rather than achieving the highest possible accuracy. Simpler probes trained on individual layers provide a more controlled setting and yield more insightful results about how linguistic information emerges throughout the network. See §C for details on classifier hyperparameters and training.

2.1.1 LINEAR REGRESSION CLASSIFIER

Consistent with best practices for probing Hewitt & Liang (2019); Liu et al. (2019), we use simple linear regression classifiers. These models are solved via closed-form ridge regression Hastie et al. (2009), using the equation:

$$W = (X_{\text{train}}^T X_{\text{train}} + \lambda I)^{-1} X_{\text{train}}^T Y_{\text{train}} \quad (1)$$

where $X_{\text{train}} \in \mathbb{R}^{m \times d}$ contains d -dimensional representations for each of the m examples in the training set, $Y_{\text{train}} \in \mathbb{R}^{m \times c}$ is the one-hot encoded matrix of training labels for c classes, λ controls the strength of L2 regularization, and $W \in \mathbb{R}^{d \times c}$ is the learned weight matrix of the classifier. Test predictions are given by:

$$\hat{Y}_{\text{test}} = X_{\text{test}} W \quad (2)$$

2.1.2 MLP CLASSIFIER

To test for more general nonlinearity, we train a simple two-layer MLP with ReLU activation, defined as:

$$\hat{Y} = \text{softmax}(\text{ReLU}(X_{\text{train}} W_1) W_2) \quad (3)$$

where $W_1 \in \mathbb{R}^{d \times h}$ and $W_2 \in \mathbb{R}^{h \times c}$ are the weight matrices and $h = 64$ is the hidden layer size (Rosenblatt, 1958).² Two-layer MLPs with ReLU activation are universal function approximators, capable of approximating any continuous function to arbitrary precision given sufficient width (Hornik et al., 1989).

Comparing performance across these classifier types provides insights into how information is encoded: if linear classifiers perform comparably to more complex probes, information is likely linearly encoded; if MLPs significantly outperform linear probes, information is non-linearly encoded (Bekinkov & Glass, 2019).

2.2 METRICS

We define several metrics for localizing where information emerges with depth and for quantifying nonlinearity: selectivity, the linear separability gap, and two depth statistics inspired by Tenney et al. (2019a), expected layer and center of gravity.

Control tasks and selectivity. Probes may simply memorize training data rather than extracting true linguistic information from the representations. To measure this, we follow Hewitt & Liang (2019) and train on randomly permuted labels (control tasks). Selectivity at layer ℓ is the difference between real and control accuracy:

$$\text{Sel}_\ell = \text{Acc}_\ell^{\text{real}} - \text{Acc}_\ell^{\text{control}} \quad (4)$$

Higher values mean the classifier is extracting true linguistic information rather than memorizing.

²Bias terms are omitted for brevity.

Linear separability gap. We quantify nonlinearity at each layer as the difference in accuracy between a non-linear probe and a linear probe:

$$\text{Gap}_\ell = \text{Acc}_\ell^{\text{nonlin}} - \text{Acc}_\ell^{\text{linear}}, \quad (5)$$

where positive values indicate useful information is present but not linearly separable; values near zero suggest linear accessibility. The gap lies in $[-1, 1]$ in principle and is typically between -0.3 and 0.3 in practice.

Center of gravity. Let a_ℓ be the test accuracy using layer ℓ for $\ell = 0, \dots, L$, and let $b_\ell = \max_{j \leq \ell} a_j$ be the cumulative (best-so-far) curve. We weight layers by their consolidation relative to the baseline and take an index-weighted average:

$$w_\ell = \frac{b_\ell - b_0}{\sum_{k=0}^L (b_k - b_0)}, \quad \text{CenterOfGravity} = \sum_{\ell=0}^L \ell w_\ell. \quad (6)$$

Higher values indicate that performance is consolidated in higher layers.

Expected layer. To localize where marginal gains arise, we use the nonnegative increments of the cumulative curve and take their index-weighted average:

$$\Delta_\ell = \max(b_\ell - b_{\ell-1}, 0), \quad p_\ell = \frac{\Delta_\ell}{\sum_{j=1}^L \Delta_j}, \quad \text{ExpectedLayer} = \sum_{\ell=1}^L \ell p_\ell. \quad (7)$$

Unlike center of gravity (which weights consolidated performance), this emphasizes where useful information first becomes available, highlighting the specific layers at which the model begins to encode properties relevant to the task.

3 EXPERIMENTS

Using the methodology introduced in §2, we describe the components of our experimental setup: the datasets, model suite, and procedure for extracting token-level representations.

3.1 DATASETS

We evaluate the eight tasks used by Tenney et al. (2019a): UD English-GUM (POS, dependencies, named entities, coreference, constituents) (Nivre et al., 2016; Zeldes, 2017), Universal Propositions English-EWT (SRL) (Jindal et al., 2022), SPR1 datasets (PropBank and UD-EWT sources; SPR), and SemEval-2010 Task 8 (relations). We use the same token/span/edge labeling schemes.

For our in-depth analysis of lexical identity and inflectional morphology, we use Universal Dependencies corpora across six languages - English, Chinese, German, French, Russian, Turkish (Nivre

Model	Parameters	Pretraining Data	Layers
Encoder-only			
BERT Base	110M	12.6B tokens ¹	12
BERT Large	340M	12.6B tokens ¹	24
DeBERTa V3 Large	418M	32B tokens ¹	24
Decoder-only			
GPT-2-Small	124M	8B tokens ¹	12
GPT-2-Large	708M	8B tokens ¹	36
GPT-2-XL	1.5B	8B tokens ¹	48
Goldfish English 1000mb	124M	200M tokens	12
Goldfish Chinese 1000mb	124M	200M tokens	12
Goldfish German 1000mb	124M	200M tokens	12
Goldfish French 1000mb	124M	200M tokens	12
Goldfish Russian 1000mb	124M	200M tokens	12
Goldfish Turkish 1000mb	124M	200M tokens	12
Pythia-6.9B	6900M	300B tokens	32
Pythia-6.9B Tulu	6900M	300B tokens	32
OLMo-2-7B	7300M	4T tokens	32
OLMo-2-7B-Instruct	7300M	4T tokens	32
Gemma-2-2B	2610M	2T tokens	26
Gemma-2-2B-Instruct	2610M	2T tokens	26
Qwen2.5-1.5B	1540M	18T tokens	28
Qwen2.5-1.5B-Instruct	1540M	18T tokens	28
Qwen2.5-7B	7620M	18T tokens	28
Qwen2.5-7B-Instruct	7620M	18T tokens	28
Llama-3.1-8B	8000M	15T tokens	32
Llama-3.1-8B-Instruct	8000M	15T tokens	32
Encoder-Decoder			
mT5-base	580M	1T tokens	12

Table 1: Overview of models used in this study

¹Converted from GB to tokens using the approximation that 1GB of data is approximately 200M tokens in English (Chang et al., 2024).

et al., 2016). We select GUM for English (Zeldes, 2017), GSD for Chinese/German/French (McDonald et al., 2013; Guillaume et al., 2019), SynTagRus for Russian (Drogaanova et al., 2018), and IMST for Turkish (Sulubacak et al., 2016).³

3.2 MODELS

We study a diverse set of pretrained transformer language models spanning different architectures, sizes, and training regimes. Table 1 lists all models used in this study (see Table 7 for the HuggingFace identifiers).

For English, we evaluate all models listed in Table 1 (excluding the non-English **Goldfish** models). For the five non-English languages (Chinese, German, French, Russian, Turkish), we focus on models that have explicit multilingual training: the **Goldfish** monolingual models trained specifically for each target language (Chang et al., 2024), multilingual Qwen2.5 variants that include these languages in their training data, and the multilingual mT5-base model (Xue et al., 2021). This ensures that we evaluate models on languages they were trained on while maintaining sufficient coverage.

3.3 REPRESENTATION EXTRACTION

We tokenize inputs with model-specific tokenizers and run a forward pass to collect residual-stream activations from every layer. Token, span, and pair encodings follow §2. For words split into multiple subwords, we use the last subword’s representation (Devlin et al., 2019). Models are used as-is (no fine-tuning), and we report results by layer using these frozen activations.

4 THE CLASSICAL NLP PIPELINE

In this section, we present probing results for eight English tasks that span the classical NLP pipeline. We report layer-wise accuracy for linear and MLP probes, summarize where each property emerges with Expected Layer and Center of Gravity, and compare models by correlating their layer-by-task accuracy profiles. All figures we show here are for three representative models; chosen to cover architecture, size and training regime. Full results for all 25 models appear in §D.

4.1 LAYER-WISE ACCURACY

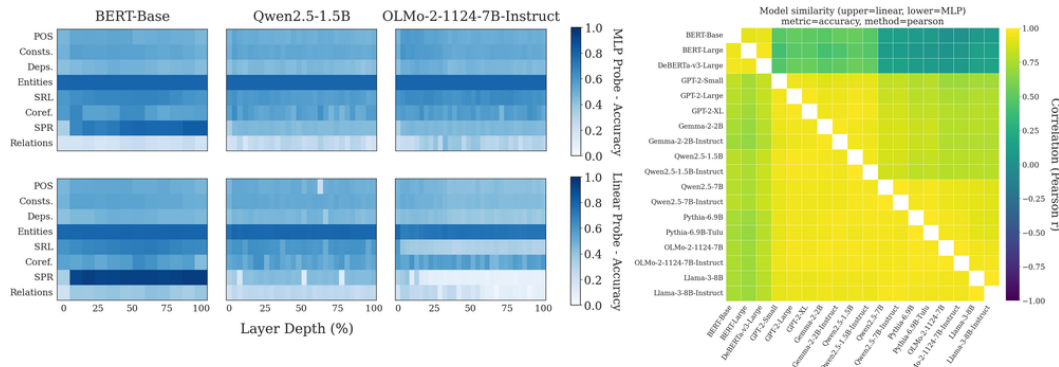


Figure 2: Left: heatmaps of probe accuracy by layer for three models (BERT-Base, Qwen2.5-1.5B, OLMo-2-1124-7B-Instruct). The top row shows MLP probe accuracy, the bottom row shows linear probe accuracy. Right: Pearson correlations between models are computed by vectorizing each model’s per-layer, per-task accuracy grid. The lower triangular matrix shows MLP probe accuracy correlations, the upper triangular matrix shows linear probe accuracy correlations.

Figure 2 shows accuracy heatmaps for three representative models and correlations between the task accuracy all models. In general, we observe high probe accuracy for tasks such as NER and low

³See §F for complete details including dataset statistics, tokenization information, and visualizations for all languages

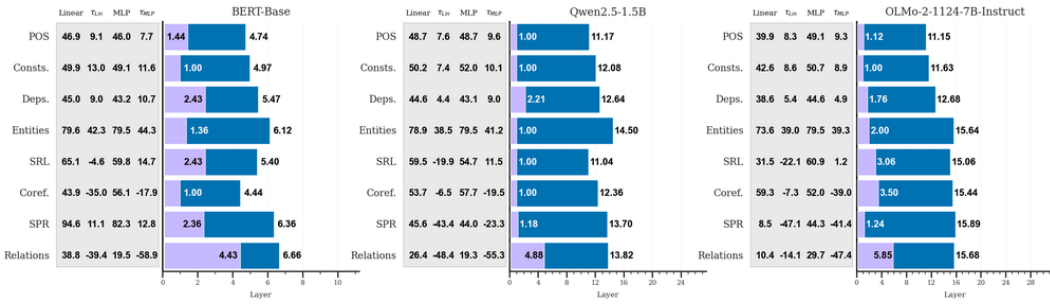


Figure 3: Expected Layer (blue, equation (7)) and Center of Gravity (purple, equation (6)) for the same three models. τ_{lin} and τ_{MLP} give selectivity (real vs. control accuracy) for linear and MLP probes. Higher τ indicates probes extract true signal rather than memorizing.

accuracy for tasks such as semantic relation extraction. Mid-level semantic tasks such as SRL and SPR peak in middle layers, while later layers capture discourse-level phenomena like Coreference and Relations. To compare results across models, we compute Pearson correlations between the task-by-layer accuracy vectors for each pair of models. We find that encoder-only models cluster together, decoder-only models form a separate cluster, and cross-family correlations are weaker. With linear probes, model size also separates clusters: small/medium decoder-only models (100M-2B) correlate strongly with each other, while 7B+ models form a distinct high-similarity group.

4.2 SUMMARY STATISTICS: EXPECTED LAYER AND CENTER OF GRAVITY

The summary statistics in Figure 3 demonstrate a more nuanced pattern. Consistent with results from Tenney et al. (2019a), we find that for early models like BERT-Base and BERT-Large, the hierarchical structure is pronounced: syntax peaks earliest, semantics and entities in the middle, and discourse phenomena latest. For larger modern models like Qwen2.5-1.5B and OLMo-2-7B-Instruct, information emerges earlier, indicated by Expected Layer values shifting toward shallower layers. These models compress multiple linguistic levels into fewer layers, perhaps reflecting stronger pretraining signals and greater model capacity. However, we still observe a hierarchical progression in center-of-gravity metrics, indicating that later layers still play a role in processing linguistic information. Selectivity scores confirm that the probe performance reflects real structure rather than memorization, especially for mid- and late-stage tasks.

4.3 DO MODERN LMs REDISCOVER THE CLASSICAL NLP PIPELINE?

Overall, our results demonstrate that modern language models consistently rediscover the classical NLP pipeline observed in prior BERTology work. Across architectures, training regimes, and model scales, we find that syntactic information is typically represented in earlier layers, semantic information becomes salient in intermediate layers, and discourse-level features are encoded most strongly in later layers. However, we also find that model capacity affects where in the network this information emerges. Smaller, earlier models such as BERT-Base exhibit the most clearly separated stages, with each linguistic property peaking at a distinct depth. As models become larger and more powerful, the peaks for different linguistic properties shift toward earlier layers, indicating that modern models learn rich representations more quickly and need fewer layers to consolidate linguistic knowledge. These findings suggest that while the hierarchical organization of linguistic information remains a robust property of language model representations, powerful models build useful representations earlier in the network.

5 LEXICAL IDENTITY AND INFLECTIONAL MORPHOLOGY

Having established that modern LMs represent the steps of the classical NLP pipeline in a hierarchical manner (§4), we now present an in-depth analysis of two token-level properties: lexical identity and inflectional morphology. We employ the same probing setup as in §4, but expand our analysis to six typologically diverse languages: English, Chinese, German, French, Russian, and Turkish. Finally,

we examine where and how these properties are encoded in model representations, including which layers make them linearly accessible.

5.1 RESULTS

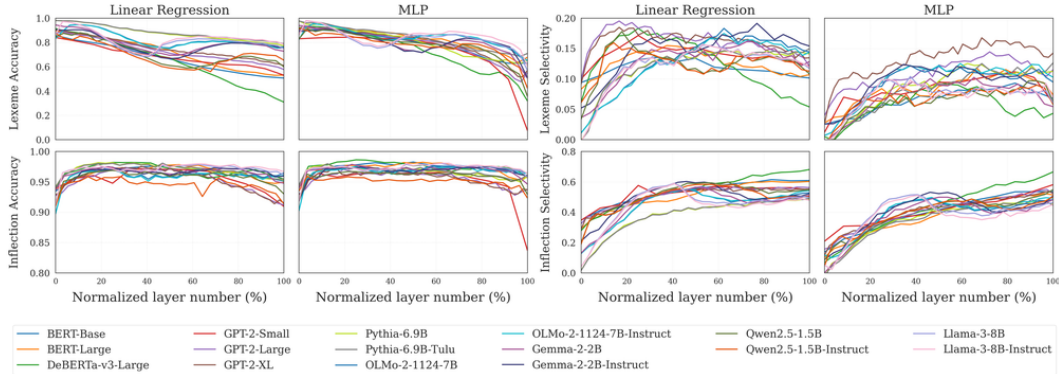


Figure 4: Linguistic accuracy and classifier selectivity across model layers for English. The first two columns show lemma (top) and inflection (bottom) prediction accuracy using Linear Regression (left) and MLP (right) classifiers. The next two columns show classifier selectivity (difference between linguistic and control task accuracy) for the same tasks and classifiers. Higher selectivity indicates better generalization rather than memorization. Each line represents a different model. Multilingual results are shown in Figure 5.

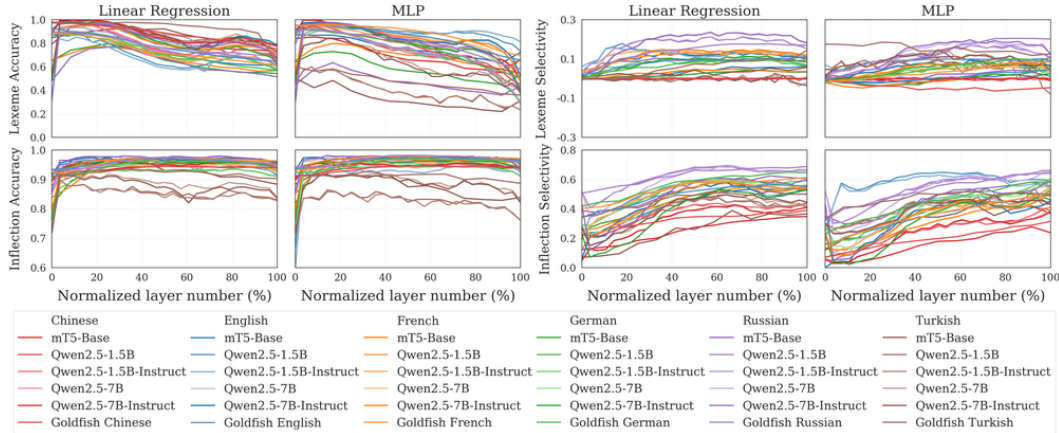


Figure 5: Cross-linguistic patterns in linguistic accuracy and classifier selectivity. The first two columns show lemma (top) and inflection (bottom) prediction accuracy using Linear Regression (left) and MLP (right) classifiers. The third column shows inflection prediction with Random Forest classifiers (lemma prediction is computationally infeasible due to the large number of classes). The rightmost columns show classifier selectivity for lemma (top) and inflection (bottom) tasks. Each line represents a different model-language combination.

We report results for lexical identity and inflectional morphology across classifier types and languages. The English set includes 19 models. We also evaluate five other languages using 6 multi/monolingual models. In addition to MLP and linear regression classifiers, we also use Random Forests for inflection (but not lemma, due to the large number of classes). Random Forest results are in §I.

5.1.1 LEMMA

Lemma task accuracy shows a sharp decline in accuracy with depth for linear regression classifiers, starting high (0.8–1.0) in the first layers and dropping in deeper layers (Figure 4, top left). The size

of the drop differs by model: DeBERTa-v3-Large falls from about 0.9 to 0.3, while Pythia-6.9B stays stronger later. By language, Turkish shows the largest decline (about 0.95 to 0.25), Russian maintains higher accuracy (about 0.6–0.8), and Chinese is in between. Two-layer MLPs raise accuracy and soften the decline (Figure 4, top middle), with Pythia models strongest across layers and GPT-2, BERT, and Qwen2.5 gaining the most from added non-linearity. Gains are largest in Turkish, suggesting that in morphologically rich languages lemma information becomes more non-linear deeper in the network. Lemma selectivity is near zero across the board, suggesting that the probes mostly memorize.

5.1.2 INFLECTIONAL MORPHOLOGY

Inflectional morphology task accuracy remains high (0.9–1.0) across layers and models for linear regression classifiers (Figure 4, bottom left), with little change with depth across architectures and languages. English, German, French, and Russian are in the 0.90–1.0 range, while Turkish is lower (about 0.85–0.92), likely due to many-suffix combinations in agglutinative morphology. Comparative and superlative adjectives are consistently hardest. MLPs match linear probes for inflection (Figure 4, bottom middle), suggesting inflection is linearly encoded. Random Forests are lower (0.65–0.90) and decline with depth, with Russian and German doing best and Turkish hardest (see §I). Using control labels, inflection shows clear selectivity (about 0.4–0.6) across models and languages, with the highest values in Russian and German. Full curves appear in Figure 4 and Figure 5 and tables in §J.

5.1.3 PROBE ERROR ANALYSIS

We also conduct an error analysis, grouping examples by part of speech and inflection type, and compare performance across frequency of occurrence. There is a clear correlation between frequency and accuracy: more frequent lemmas and inflections yield higher accuracy, particularly for lemmas, with rare words consistently the hardest. Among inflection types, comparative and superlative degrees, as well as low-count verb forms, exhibit the highest error rates across models. These trends are consistent across languages, with Turkish showing the strongest sensitivity to frequency. Detailed tables and plots are provided in §J.

5.2 ANALYSIS

Our experiments demonstrate clear patterns in how models process lexical identity and inflectional morphology. Here, we explore further and analyze six key aspects of these representations: cross-linguistic trends, representation structure, attention head outputs vs. residual stream, training dynamics, steering experiments, and intrinsic dimensionality.

Cross-Linguistic Trends Across six languages, lemma is most readable early and declines with depth, while inflection stays high across layers (Figure 5). Turkish shows the steepest lemma drop; Russian stays highest overall. These trends align with reports that agglutinative systems challenge current LMs.

Linear Representations We compare linear probes with two-layer MLPs using the linear separability gap from §2. For inflection, gaps are near zero (sometimes slightly positive or negative), indicating that a linear map already captures most of the signal. For lemma, gaps are negative in early layers and shrink later, reflecting that regularized linear regression often outperforms a small MLP, especially where lexical information is concentrated and strongly tied to item frequency.

Intrinsic Dimensionality To characterize how representations evolve through depth, we measure intrinsic dimensionality with PCA (Table 2 and Figure 11). Models fall into two groups: some show gradual dimensionality decline (BERT, DeBERTa, Gemma, Llama 3.1), while others have middle layers where a single component explains most variance (GPT-2, Qwen2.5, Pythia, OLMo-2). Some families show gradual decline with depth; others have highly compressed mid-layers. Low intrinsic dimensionality has practical implications: we show below that steering vectors can more effectively manipulate model behavior by targeting compressed middle-layer representations.

Attention vs. Residual Stream Comparing averaged attention head outputs to the residual stream, lemma information drops in attention outputs in middle layers while the residual stream stays higher. Inflection remains strong in both, with the residual stream slightly better in the middle. This supports the view that attention focuses on contextual relations, while MLP blocks store more parametric knowledge. See §G.

Training Dynamics We evaluate checkpoints for OLMo-2-7B and Pythia-6.9B. Three patterns emerge. First, the split between lemma and inflection appears early: lemma accuracy peaks at early steps and declines gradually with more training, while inflection accuracy is high and flat from the start. Second, the layer at which lemma is most readable shifts slightly toward earlier layers as training proceeds, consistent with increasing contextualization in middle and late layers. Third, these trends hold across both families despite different corpora and training scales, pointing to architecture-level behavior rather than a dataset artifact. Figures are in Figures 24 and 25.

Steering Experiments We apply steering vectors computed from class means for inflection categories and test several strengths. Steering is effective across most layers and models: mean probability change and flip rates are near 1.0 in many regions, showing that inflectional directions are functionally manipulable. The models which are least steerable are the same ones which have a low intrinsic dimensionality in mid-layers, suggesting that compressed representations are harder to adjust with simple vector shifts. See §H for full details.

6 RELATED WORK

Probing for linguistic information Probing studies typically use supervised classifiers to predict linguistic properties from model representations (Alain & Bengio, 2017; Adi et al., 2017). Extensive work has established that early transformer models (BERT, GPT-2) learn hierarchical linguistic structures, with different layers specializing in different information types: lower layers capture surface features and morphology, middle layers encode syntax, and upper layers represent semantics and context (Jawahar et al., 2019; Tenney et al., 2019a; Rogers et al., 2020). More relevant to our work, Vulić et al. (2020) found that lexical information concentrates in lower layers, while Ethayarajh (2019) showed that representations become increasingly context-specific in higher layers.

Activation steering Beyond probing, recent work has explored manipulating model behavior by intervening on internal representations. This includes steering vectors (Subramani et al., 2022), inference-time interventions (Li et al., 2023), representation editing (Meng et al., 2022), sparse autoencoders for feature discovery (Bricken et al., 2023), and causal mediation analysis (Vig et al., 2020). While these methods typically evaluate changes in model outputs, our steering experiments focus on measuring representational changes. See §B for more detailed discussion.

7 CONCLUSION

In this paper, we examined 25 transformer models and found evidence that modern LMs rediscover the classical NLP pipeline: syntax is most accessible first, then semantic and entity-level information, and finally discourse. At the same time, we observe that larger contemporary models shift these peaks toward earlier layers, suggesting that stronger capacity and training lead to useful representations emerging sooner. Our in-depth study of lexical identity and inflectional morphology shows a clear pattern. Lemma information concentrates early and becomes increasingly non-linear with depth, while inflectional features remain linearly accessible throughout layers and across languages. Analyses of attention vs. residual streams, pretraining checkpoints, and steering vectors further locate where this information lives, when it appears, and how it can be manipulated. These results hold across architectures, sizes, and training regimes, pointing to robust representational regularities that persist despite rapid advances in model scale and training practice.

8 REPRODUCIBILITY STATEMENT

Our GitHub repository is available at https://github.com/m15885/model_internal_sleuthing. It contains code to reproduce dataset construction, probing experiments, and all plots and analyses. The

main paper specifies the probe design and metrics (§2), datasets and model suite (§3 and Table 1), and evaluation summaries for the classical pipeline and for lexical identity and inflectional morphology (§4 and §5). The appendix provides complete classifier and training details, dataset statistics, and full-resolution figure grids referenced in the text. Together, these materials are intended to enable end-to-end reproduction of our results.

REFERENCES

Yossi Adi, Einat Kermany, Yonatan Belinkov, Ofer Lavi, and Yoav Goldberg. Fine-grained analysis of sentence embeddings using auxiliary prediction tasks. In *5th International Conference on Learning Representations (Conference Track)*, 2017. URL <https://openreview.net/forum?id=Bjh6Ztux1>.

Guillaume Alain and Yoshua Bengio. Understanding intermediate layers using linear classifier probes. In *5th International Conference on Learning Representations (Workshop Track)*, 2017. URL <https://openreview.net/forum?id=ryF7rTqgl>.

Yonatan Belinkov and James Glass. Analysis methods in neural language processing: A survey. *Transactions of the Association for Computational Linguistics*, 7:49–72, 2019. doi: 10.1162/tacl_a_00254. URL <https://aclanthology.org/Q19-1004/>.

Leo Breiman. Random forests. *Mach. Learn.*, 45(1):5–32, October 2001. ISSN 0885-6125. doi: 10.1023/A:1010933404324. URL <https://doi.org/10.1023/A:1010933404324>.

Trenton Bricken, Adly Templeton, Joshua Batson, Brian Chen, Adam Jermyn, Tom Conerly, Nick Turner, Cem Anil, Carson Denison, Amanda Askell, Robert Lasenby, Yifan Wu, Shauna Kravec, Nicholas Schiefer, Tim Maxwell, Nicholas Joseph, Zac Hatfield-Dodds, Alex Tamkin, Karina Nguyen, Brayden McLean, Josiah E Burke, Tristan Hume, Shan Carter, Tom Henighan, and Christopher Olah. Towards monosematicity: Decomposing language models with dictionary learning. *Transformer Circuits Thread*, 2023. <https://transformer-circuits.pub/2023/monosemantic-features/index.html>.

Tom B. Brown, Benjamin Mann, Nick Ryder, Melanie Subbiah, Jared Kaplan, Prafulla Dhariwal, Arvind Neelakantan, Pranav Shyam, Girish Sastry, Amanda Askell, Sandhini Agarwal, Ariel Herbert-Voss, Gretchen Krueger, Tom Henighan, Rewon Child, Aditya Ramesh, Daniel M. Ziegler, Jeffrey Wu, Clemens Winter, Christopher Hesse, Mark Chen, Eric Sigler, Mateusz Litwin, Scott Gray, Benjamin Chess, Jack Clark, Christopher Berner, Sam McCandlish, Alec Radford, Ilya Sutskever, and Dario Amodei. Language models are few-shot learners, 2020. URL <https://arxiv.org/abs/2005.14165>.

Tyler A. Chang, Catherine Arnett, Zhuowen Tu, and Benjamin K. Bergen. Goldfish: Monolingual language models for 350 languages, 2024. URL <https://arxiv.org/abs/2408.10441>.

Hoagy Cunningham, Aidan Ewart, Logan Riggs, Robert Huben, and Lee Sharkey. Sparse autoencoders find highly interpretable features in language models, 2023. URL <https://arxiv.org/abs/2309.08600>.

Thao Anh Dang, Limor Raviv, and Lukas Galke. Tokenization and morphology in multilingual language models: A comparative analysis of mt5 and byt5, 2024. URL <https://arxiv.org/abs/2410.11627>.

Jacob Devlin, Ming-Wei Chang, Kenton Lee, and Kristina Toutanova. BERT: Pre-training of deep bidirectional transformers for language understanding. In Jill Burstein, Christy Doran, and Thamar Solorio (eds.), *Proceedings of the 2019 Conference of the North American Chapter of the Association for Computational Linguistics: Human Language Technologies, Volume 1 (Long and Short Papers)*, pp. 4171–4186, Minneapolis, Minnesota, June 2019. Association for Computational Linguistics. doi: 10.18653/v1/N19-1423. URL <https://aclanthology.org/N19-1423/>.

Kira Droganova, Olga Lyshevskaya, and Daniel Zeman. Data conversion and consistency of monolingual corpora: Russian ud treebanks. In *Proceedings of the 17th international workshop on treebanks and linguistic theories (ltl 2018)*, volume 155, pp. 53–66. Linköping University Electronic Press Linköping, Sweden, 2018.

Yanai Elazar, Shauli Ravfogel, Alon Jacovi, and Yoav Goldberg. Amnesic Probing: Behavioral Explanation with Amnesic Counterfactuals. *Transactions of the Association for Computational Linguistics*, 9:160–175, 03 2021. ISSN 2307-387X. doi: 10.1162/tacl_a_00359. URL https://doi.org/10.1162/tacl_a_00359.

Nelson Elhage, Neel Nanda, Catherine Olsson, Tom Henighan, Nicholas Joseph, Ben Mann, Amanda Askell, Yuntao Bai, Anna Chen, Tom Conerly, Nova DasSarma, Dawn Drain, Deep Ganguli, Zac Hatfield-Dodds, Danny Hernandez, Andy Jones, Jackson Kernion, Liane Lovitt, Kamal Ndousse, Dario Amodei, Tom Brown, Jack Clark, Jared Kaplan, Sam McCandlish, and Chris Olah. A mathematical framework for transformer circuits. *Transformer Circuits Thread*, 2021. <https://transformer-circuits.pub/2021/framework/index.html>.

Kawin Ethayarajh. How contextual are contextualized word representations? Comparing the geometry of BERT, ELMo, and GPT-2 embeddings. In Kentaro Inui, Jing Jiang, Vincent Ng, and Xiaojun Wan (eds.), *Proceedings of the 2019 Conference on Empirical Methods in Natural Language Processing and the 9th International Joint Conference on Natural Language Processing (EMNLP-IJCNLP)*, pp. 55–65, Hong Kong, China, November 2019. Association for Computational Linguistics. doi: 10.18653/v1/D19-1006. URL <https://aclanthology.org/D19-1006/>.

Atticus Geiger, Hanson Lu, Thomas F Icard, and Christopher Potts. Causal abstractions of neural networks. In A. Beygelzimer, Y. Dauphin, P. Liang, and J. Wortman Vaughan (eds.), *Advances in Neural Information Processing Systems*, 2021. URL <https://openreview.net/forum?id=RmuXDtjDhG>.

Dirk Groeneveld, Iz Beltagy, Evan Walsh, Akshita Bhagia, Rodney Kinney, Oyvind Tafjord, Ananya Jha, Hamish Ivison, Ian Magnusson, Yizhong Wang, Shane Arora, David Atkinson, Russell Arthur, Khyathi Chandu, Arman Cohan, Jennifer Dumas, Yanai Elazar, Yuling Gu, Jack Hessel, Tushar Khot, William Merrill, Jacob Morrison, Niklas Muennighoff, Aakanksha Naik, Crystal Nam, Matthew Peters, Valentina Pyatkin, Abhilasha Ravichander, Dustin Schwenk, Saurabh Shah, William Smith, Emma Strubell, Nishant Subramani, Mitchell Wortsman, Pradeep Dasigi, Nathan Lambert, Kyle Richardson, Luke Zettlemoyer, Jesse Dodge, Kyle Lo, Luca Soldaini, Noah Smith, and Hannaneh Hajishirzi. OLMo: Accelerating the science of language models. In Lun-Wei Ku, Andre Martins, and Vivek Srikumar (eds.), *Proceedings of the 62nd Annual Meeting of the Association for Computational Linguistics (Volume 1: Long Papers)*, pp. 15789–15809, Bangkok, Thailand, August 2024. Association for Computational Linguistics. doi: 10.18653/v1/2024.acl-long.841. URL <https://aclanthology.org/2024.acl-long.841/>.

Bruno Guillaume, Marie-Catherine de Marneffe, and Guy Perrier. Conversion et améliorations de corpus du français annotés en Universal Dependencies [conversion and improvement of Universal Dependencies French corpora]. *Traitemet Automatique des Langues*, 60(2):71–95, 2019. URL <https://aclanthology.org/2019.tal-2.4/>.

Trevor Hastie, Robert Tibshirani, and Jerome Friedman. *The Elements of Statistical Learning: Data Mining, Inference, and Prediction*. Springer, New York, NY, USA, 2 edition, 2009. ISBN 978-0-387-84857-0. URL <https://web.stanford.edu/~hastie/ElemStatLearn/>.

John Hewitt and Percy Liang. Designing and interpreting probes with control tasks. In Kentaro Inui, Jing Jiang, Vincent Ng, and Xiaojun Wan (eds.), *Proceedings of the 2019 Conference on Empirical Methods in Natural Language Processing and the 9th International Joint Conference on Natural Language Processing (EMNLP-IJCNLP)*, pp. 2733–2743, Hong Kong, China, November 2019. Association for Computational Linguistics. doi: 10.18653/v1/D19-1275. URL <https://aclanthology.org/D19-1275/>.

Kurt Hornik, Maxwell Stinchcombe, and Halbert White. Multilayer feedforward networks are universal approximators. *Neural Networks*, 2(5):359–366, 1989. ISSN 0893-6080. doi: [https://doi.org/10.1016/0893-6080\(89\)90020-8](https://doi.org/10.1016/0893-6080(89)90020-8). URL <https://www.sciencedirect.com/science/article/pii/0893608089900208>.

Binyuan Hui, Jian Yang, Zeyu Cui, Jiaxi Yang, Dayiheng Liu, Lei Zhang, Tianyu Liu, Jiajun Zhang, Bowen Yu, Kai Dang, et al. Qwen2. 5-coder technical report. *arXiv preprint arXiv:2409.12186*, 2024.

Gabriel Ilharco, Marco Túlio Ribeiro, Mitchell Wortsman, Ludwig Schmidt, Hannaneh Hajishirzi, and Ali Farhadi. Editing models with task arithmetic. In *The Eleventh International Conference on Learning Representations*, 2023. URL <https://openreview.net/forum?id=6t0Kwf8-jrj>.

Ganesh Jawahar, Benoît Sagot, and Djamé Seddah. What does BERT learn about the structure of language? In Anna Korhonen, David Traum, and Lluís Màrquez (eds.), *Proceedings of the 57th Annual Meeting of the Association for Computational Linguistics*, pp. 3651–3657, Florence, Italy, July 2019. Association for Computational Linguistics. doi: 10.18653/v1/P19-1356. URL <https://aclanthology.org/P19-1356/>.

Ishan Jindal, Alexandre Rademaker, Michał Ulewicz, Ha Linh, Huyen Nguyen, Khoi-Nguyen Tran, Huaiyu Zhu, and Yunyao Li. Universal Proposition Bank 2.0. In Nicoletta Calzolari, Frédéric Béchet, Philippe Blache, Khalid Choukri, Christopher Cieri, Thierry Declerck, Sara Goggi, Hitoshi Isahara, Bente Maegaard, Joseph Mariani, Hélène Mazo, Jan Odijk, and Stelios Piperidis (eds.), *Proceedings of the Thirteenth Language Resources and Evaluation Conference*, pp. 1700–1711, Marseille, France, June 2022. European Language Resources Association. URL <https://aclanthology.org/2022.lrec-1.181/>.

Diederik P Kingma and Jimmy Ba. Adam: A method for stochastic optimization. *arXiv preprint arXiv:1412.6980*, 2014.

Nathan Lambert, Jacob Morrison, Valentina Pyatkin, Shengyi Huang, Hamish Ivison, Faeze Brahman, Lester James V. Miranda, Alisa Liu, Nouha Dziri, Shane Lyu, Yuling Gu, Saumya Malik, Victoria Graf, Jena D. Hwang, Jiangjiang Yang, Ronan Le Bras, Oyvind Tafjord, Chris Wilhelm, Luca Soldaini, Noah A. Smith, Yizhong Wang, Pradeep Dasigi, and Hannaneh Hajishirzi. Tulu 3: Pushing frontiers in open language model post-training, 2025. URL <https://arxiv.org/abs/2411.15124>.

Kenneth Li, Oam Patel, Fernanda Viégas, Hanspeter Pfister, and Martin Wattenberg. Inference-time intervention: Eliciting truthful answers from a language model. In *Thirty-seventh Conference on Neural Information Processing Systems*, 2023. URL <https://openreview.net/forum?id=aLLuYpn83y>.

Nelson F. Liu, Matt Gardner, Yonatan Belinkov, Matthew E. Peters, and Noah A. Smith. Linguistic knowledge and transferability of contextual representations. In Jill Burstein, Christy Doran, and Thamar Solorio (eds.), *Proceedings of the 2019 Conference of the North American Chapter of the Association for Computational Linguistics: Human Language Technologies, Volume 1 (Long and Short Papers)*, pp. 1073–1094, Minneapolis, Minnesota, June 2019. Association for Computational Linguistics. doi: 10.18653/v1/N19-1112. URL <https://aclanthology.org/N19-1112/>.

Team Llama. The llama 3 herd of models, 2024. URL <https://arxiv.org/abs/2407.21783>.

Ryan McDonald, Joakim Nivre, Yvonne Quirmbach-Brundage, Yoav Goldberg, Dipanjan Das, Kuzman Ganchev, Keith Hall, Slav Petrov, Hao Zhang, Oscar Täckström, Claudia Bedini, Núria Bertomeu Castelló, and Jungmee Lee. Universal Dependency annotation for multilingual parsing. In Hinrich Schuetze, Pascale Fung, and Massimo Poesio (eds.), *Proceedings of the 51st Annual Meeting of the Association for Computational Linguistics (Volume 2: Short Papers)*, pp. 92–97, Sofia, Bulgaria, August 2013. Association for Computational Linguistics. URL <https://aclanthology.org/P13-2017/>.

Kevin Meng, David Bau, Alex J Andonian, and Yonatan Belinkov. Locating and editing factual associations in GPT. In Alice H. Oh, Alekh Agarwal, Danielle Belgrave, and Kyunghyun Cho (eds.), *Advances in Neural Information Processing Systems*, 2022. URL <https://openreview.net/forum?id=-h6WAS6eE4>.

Joakim Nivre, Marie-Catherine de Marneffe, Filip Ginter, Yoav Goldberg, Jan Hajič, Christopher D. Manning, Ryan McDonald, Slav Petrov, Sampo Pyysalo, Natalia Silveira, Reut Tsarfaty, and Daniel Zeman. Universal Dependencies v1: A multilingual treebank collection. In Nicoletta Calzolari, Khalid Choukri, Thierry Declerck, Sara Goggi, Marko Grobelnik, Bente Maegaard, Joseph Mariani, Helene Mazo, Asuncion Moreno, Jan Odijk, and Stelios Piperidis (eds.), *Proceedings of the Tenth International Conference on Language Resources and Evaluation (LREC'16)*, pp.

1659–1666, Portorož, Slovenia, May 2016. European Language Resources Association (ELRA). URL <https://aclanthology.org/L16-1262/>.

nostalgebraist. interpreting gpt: the logit lens, Aug 2020. URL <https://www.lesswrong.com/posts/AcKRB8wDpdaN6v6ru/interpreting-gpt-the-logit-lens>.

Nina Panickssery, Nick Gabrieli, Julian Schulz, Meg Tong, Evan Hubinger, and Alexander Matt Turner. Steering llama 2 via contrastive activation addition, 2024. URL <https://arxiv.org/abs/2312.06681>.

F. Pedregosa, G. Varoquaux, A. Gramfort, V. Michel, B. Thirion, O. Grisel, M. Blondel, P. Prettenhofer, R. Weiss, V. Dubourg, J. Vanderplas, A. Passos, D. Cournapeau, M. Brucher, M. Perrot, and E. Duchesnay. Scikit-learn: Machine learning in Python. *Journal of Machine Learning Research*, 12:2825–2830, 2011.

Alec Radford, Jeff Wu, Rewon Child, David Luan, Dario Amodei, and Ilya Sutskever. Language models are unsupervised multitask learners. *OpenAI blog*, 1(8):9, 2019.

Anna Rogers, Olga Kovaleva, and Anna Rumshisky. A primer in BERTology: What we know about how BERT works. *Transactions of the Association for Computational Linguistics*, 8:842–866, 2020. doi: 10.1162/tacl_a_00349. URL <https://aclanthology.org/2020.tacl-1.54/>.

Frank Rosenblatt. The perceptron: a probabilistic model for information storage and organization in the brain. *Psychological review*, 65(6):386, 1958.

Nishant Subramani, Nivedita Suresh, and Matthew Peters. Extracting latent steering vectors from pretrained language models. In Smaranda Muresan, Preslav Nakov, and Aline Villavicencio (eds.), *Findings of the Association for Computational Linguistics: ACL 2022*, pp. 566–581, Dublin, Ireland, May 2022. Association for Computational Linguistics. doi: 10.18653/v1/2022.findings-acl.48. URL <https://aclanthology.org/2022.findings-acl.48/>.

Nishant Subramani, Jason Eisner, Justin Svegliato, Benjamin Van Durme, Yu Su, and Sam Thomson. MICE for CATs: Model-internal confidence estimation for calibrating agents with tools. In Luis Chiruzzo, Alan Ritter, and Lu Wang (eds.), *Proceedings of the 2025 Conference of the Nations of the Americas Chapter of the Association for Computational Linguistics: Human Language Technologies (Volume 1: Long Papers)*, pp. 12362–12375, Albuquerque, New Mexico, April 2025. Association for Computational Linguistics. ISBN 979-8-89176-189-6. URL <https://aclanthology.org/2025.naacl-long.615/>.

Umut Sulubacak, Memduh Gokirmak, Francis Tyers, Çağrı Çöltekin, Joakim Nivre, and Gülsen Eryiğit. Universal Dependencies for Turkish. In Yuji Matsumoto and Rashmi Prasad (eds.), *Proceedings of COLING 2016, the 26th International Conference on Computational Linguistics: Technical Papers*, pp. 3444–3454, Osaka, Japan, December 2016. The COLING 2016 Organizing Committee. URL <https://aclanthology.org/C16-1325/>.

Ian Tenney, Dipanjan Das, and Ellie Pavlick. BERT rediscovers the classical NLP pipeline. In Anna Korhonen, David Traum, and Lluís Márquez (eds.), *Proceedings of the 57th Annual Meeting of the Association for Computational Linguistics*, pp. 4593–4601, Florence, Italy, July 2019a. Association for Computational Linguistics. doi: 10.18653/v1/P19-1452. URL <https://aclanthology.org/P19-1452/>.

Ian Tenney, Patrick Xia, Berlin Chen, Alex Wang, Adam Poliak, R Thomas McCoy, Najoung Kim, Benjamin Van Durme, Sam Bowman, Dipanjan Das, and Ellie Pavlick. What do you learn from context? probing for sentence structure in contextualized word representations. In *International Conference on Learning Representations*, 2019b. URL <https://openreview.net/forum?id=SJzSgnRcKX>.

Jesse Vig, Sebastian Gehrmann, Yonatan Belinkov, Sharon Qian, Daniel Nevo, Yaron Singer, and Stuart Shieber. Investigating gender bias in language models using causal mediation analysis. In H. Larochelle, M. Ranzato, R. Hadsell, M.F. Balcan, and H. Lin (eds.), *Advances in Neural Information Processing Systems*, volume 33, pp. 12388–12401. Curran Associates, Inc., 2020. URL https://proceedings.neurips.cc/paper_files/paper/2020/file/92650b2e92217715fe312e6fa7b90d82-Paper.pdf.

Elena Voita and Ivan Titov. Information-theoretic probing with minimum description length. In Bonnie Webber, Trevor Cohn, Yulan He, and Yang Liu (eds.), *Proceedings of the 2020 Conference on Empirical Methods in Natural Language Processing (EMNLP)*, pp. 183–196, Online, November 2020. Association for Computational Linguistics. doi: 10.18653/v1/2020.emnlp-main.14. URL <https://aclanthology.org/2020.emnlp-main.14/>.

Ivan Vulić, Edoardo Maria Ponti, Robert Litschko, Goran Glavaš, and Anna Korhonen. Probing pretrained language models for lexical semantics. In Bonnie Webber, Trevor Cohn, Yulan He, and Yang Liu (eds.), *Proceedings of the 2020 Conference on Empirical Methods in Natural Language Processing (EMNLP)*, pp. 7222–7240, Online, November 2020. Association for Computational Linguistics. doi: 10.18653/v1/2020.emnlp-main.586. URL <https://aclanthology.org/2020.emnlp-main.586/>.

BigScience Workshop. Bloom: A 176b-parameter open-access multilingual language model, 2023. URL <https://arxiv.org/abs/2211.05100>.

Linting Xue, Noah Constant, Adam Roberts, Mihir Kale, Rami Al-Rfou, Aditya Siddhant, Aditya Barua, and Colin Raffel. mT5: A massively multilingual pre-trained text-to-text transformer. In Kristina Toutanova, Anna Rumshisky, Luke Zettlemoyer, Dilek Hakkani-Tur, Iz Beltagy, Steven Bethard, Ryan Cotterell, Tanmoy Chakraborty, and Yichao Zhou (eds.), *Proceedings of the 2021 Conference of the North American Chapter of the Association for Computational Linguistics: Human Language Technologies*, pp. 483–498, Online, June 2021. Association for Computational Linguistics. doi: 10.18653/v1/2021.naacl-main.41. URL <https://aclanthology.org/2021.naacl-main.41/>.

Amir Zeldes. The GUM corpus: Creating multilayer resources in the classroom. *Language Resources and Evaluation*, 51(3):581–612, 2017. doi: <http://dx.doi.org/10.1007/s10579-016-9343-x>.

A LIMITATIONS

Representation Extraction for Decoder Models Our current approach for extracting word representations from decoder-only models uses the final subword token. This assumption is an intuitive and natural choice, but may not be optimal for all architectures and models. Future work could develop better extraction methods that account for subword tokenization effects and leverage attention patterns to create more accurate word-level representations.

Form and Function in Inflection Some languages contain cases where different grammatical functions share the same surface form (*e.g.*, , infinitive and non-past verb forms in English). We do not explicitly examine these cases in our classification experiments, but these ambiguities create opportunities to better examine how models separate form from function across languages.

Indirect Nature of Classifiers While our classifier methodology follows established best practices (Hewitt & Liang, 2019; Liu et al., 2019), we only detect correlations in hidden activations, not causal mechanisms.

Scope of Steering Experiments Our steering vector experiments measure changes in classifier performance rather than downstream model outputs. Evaluating effects on actual model generation would require more complex experimental designs to control for confounding factors and ensure that observed changes result from the intended representational modifications rather than other influences.

B ADDITIONAL RELATED WORK

B.1 ADVANCED PROBING METHODOLOGIES

Beyond standard linear probes, there are many sophisticated approaches to understand model representations. Amnesic probing (Elazar et al., 2021) removes specific information from representations to test whether it’s necessary for downstream tasks. Minimum description length probes (Voita & Titov, 2020) balance probe complexity with performance to avoid overfitting. Causal probing (Geiger et al., 2021) aims to establish causal rather than merely correlational relationships between representations and linguistic properties. Recently, Subramani et al. (2025) find that decoding from activations directly using the Logit Lens can be used to learn confidence estimators for tool-calling agents (nostalggebraist, 2020).

B.2 MODEL MANIPULATION AND STEERING

Steering vectors demonstrate that specific directions in activation space correspond to high-level behavioral changes (Subramani et al., 2022). Building on this, Panickssery et al. (2024) achieves behavioral control by adding activation differences between contrasting examples. Li et al. (2023) introduce inference-time intervention, a method that shifts model activations during inference across limited attention heads to control model behavior. While these methods operate in activation space, task vectors enable arithmetic operations on model capabilities by manipulating weight space (Ilharco et al., 2023).

Recent work has also examined how multilingual models like mT5 and ByT5 encode morphological information differently across languages (Dang et al., 2024), finding that tokenization strategies significantly impact morphological representation quality, particularly for morphologically rich languages.

B.3 FEATURE DISCOVERY AND MECHANISTIC INTERPRETABILITY

Recent work has explored using sparse autoencoders to discover latent features (Cunningham et al., 2023; Bricken et al., 2023), providing clearer targets for steering and interpretation. Mechanistic interpretability approaches aim to reverse-engineer the algorithms learned by neural networks (Elhage et al., 2021). Representation editing directly modifies model weights to alter specific factual associations (Meng et al., 2022). These methods complement classification-based approaches by identifying the underlying structure of learned representations and their functional significance.

C TRAINING DETAILS

We stratify all datasets into train, validation and test splits. We train classifiers using the training set, select hyperparameters using the validation set, and evaluate on the held-out test set using accuracy and macro F1. For linear regression, we use ridge regularization with $\lambda = 0.01$. For random forests, we tune the number of trees (50, 100, 200) and maximum depth (5, 10, 20, None) using grid search. For MLPs, we use a hidden layer size of 64, learning rate of 0.001, weight decay of 0.01, and train for up to 100 epochs with early stopping based on validation loss. We solve equation (1) in closed-form to identify $W \in \mathbb{R}^{d \times c}$, and learn W_1 and W_2 for the MLP via stochastic gradient descent using the AdamW optimizer on cross-entropy loss (Kingma & Ba, 2014). ⁴proximators, capable of approximating any continuous function to arbitrary precision given sufficient width (Hornik et al., 1989).

D FULL RESULTS FOR THE CLASSICAL NLP PIPELINE

⁴We use weight decay for regularization for MLP models.

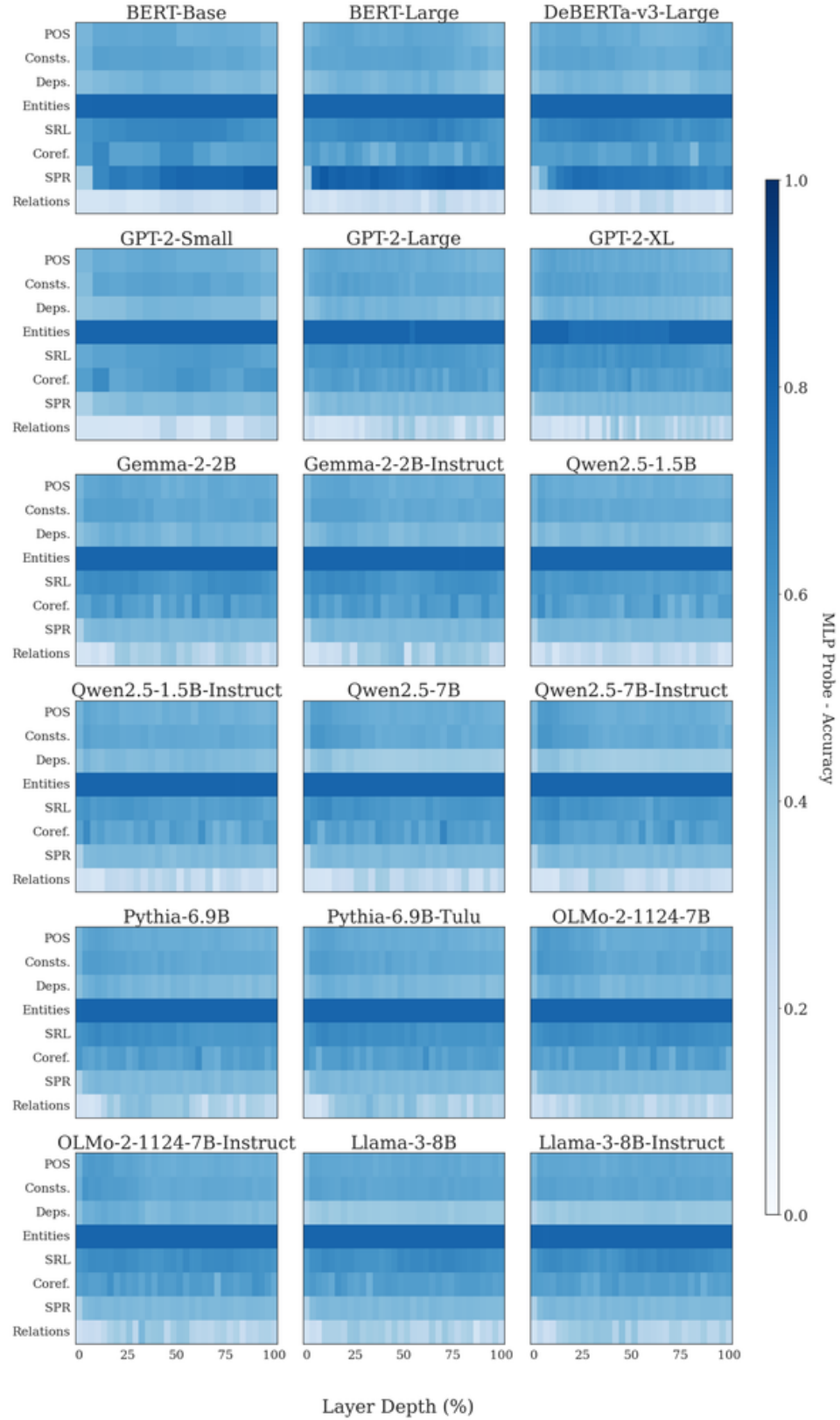


Figure 6: Full heatmaps for MLP probe accuracy across all tasks, models, and layers. Rows show tasks; columns show models; each cell shows accuracy by layer depth. Early layers favor syntax, middle layers semantics, late layers discourse.

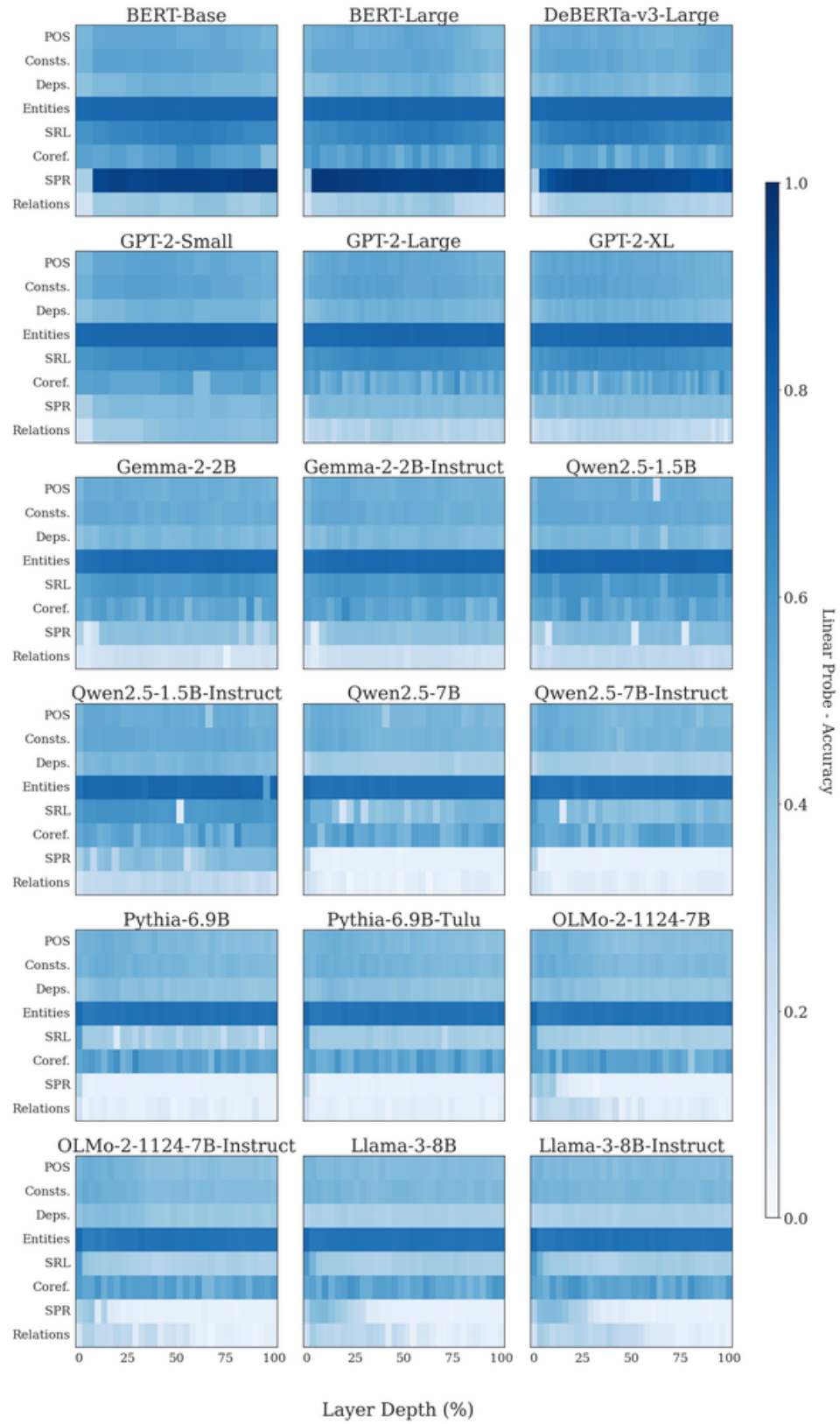


Figure 7: Full heatmaps for linear probe accuracy across all tasks, models, and layers. Trends mirror the MLP version but with stronger model-size effects in deeper layers.

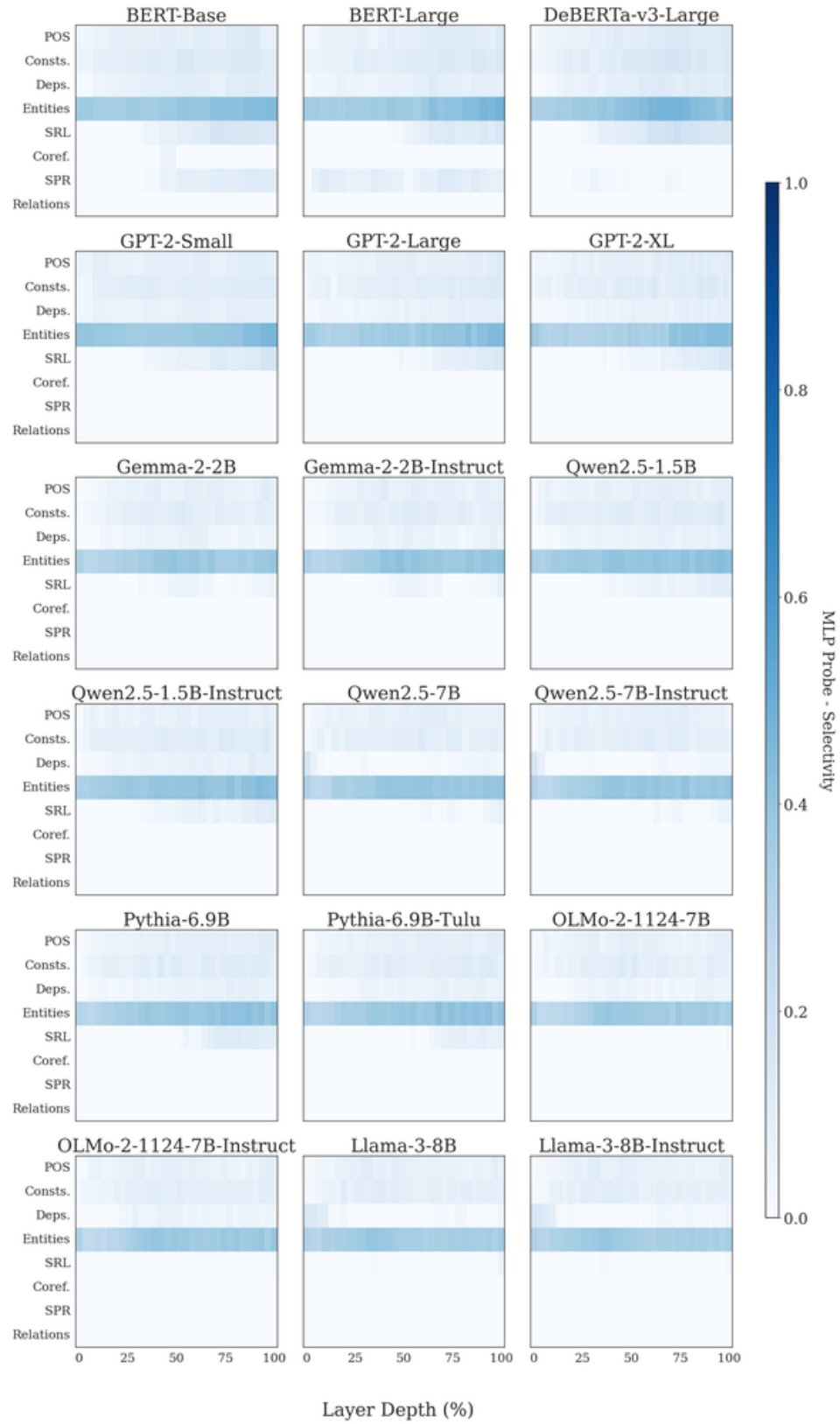


Figure 8: Full heatmaps for MLP probe selectivity (real vs. control task accuracy). Higher values indicate true signal rather than memorization.

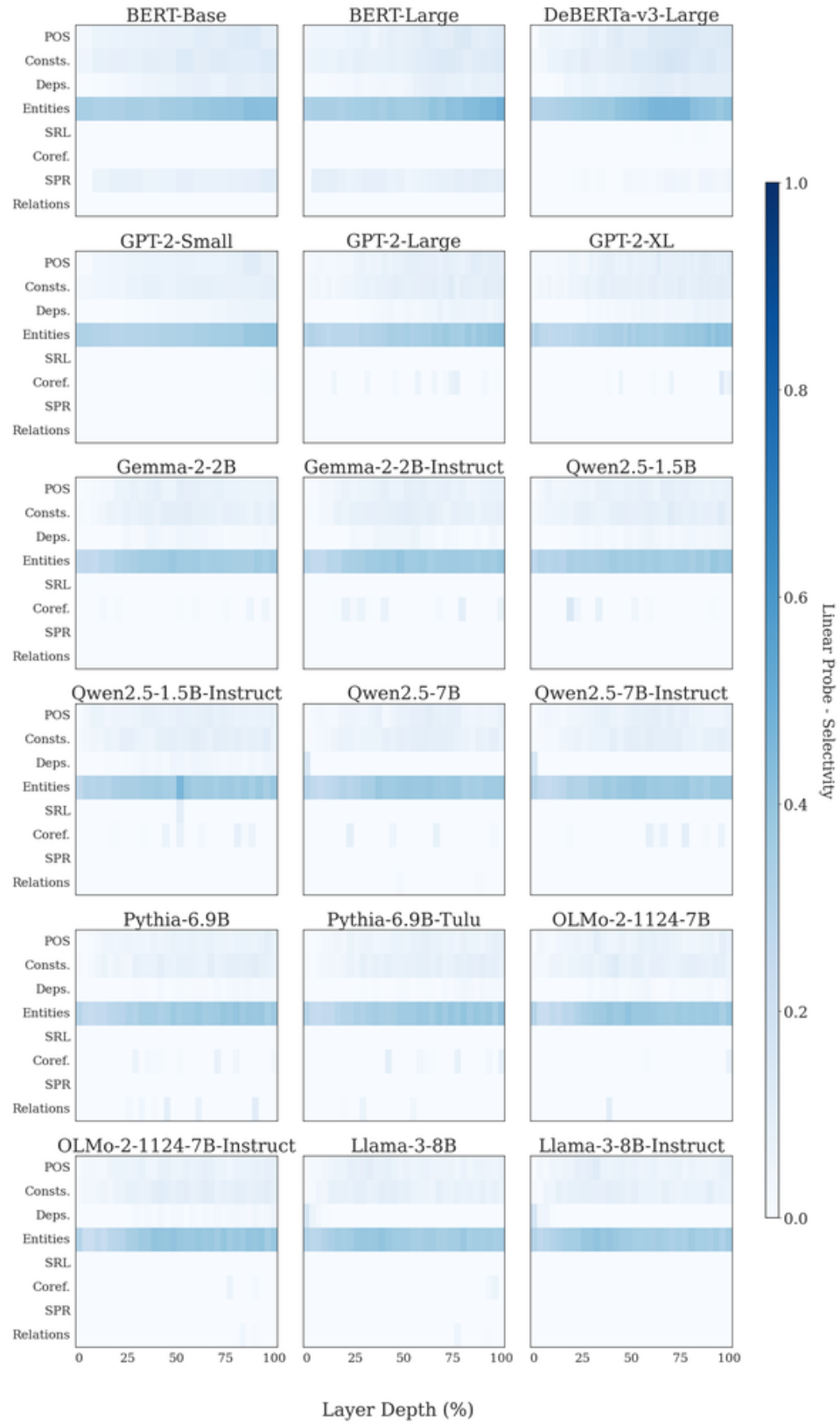


Figure 9: Full heatmaps for linear probe selectivity (real vs. control task accuracy). Selectivity is generally higher for semantic and discourse tasks.

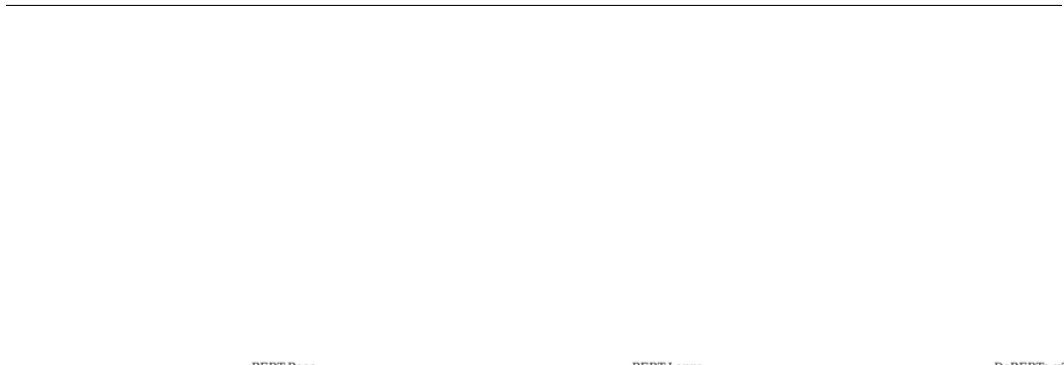


Figure 10: Full Expected Layer and Center of Gravity plots with τ_{lin} and τ_{MLP} selectivity scores for all models. We observe early peaks for syntax, middle peaks for semantics, and late peaks for discourse across architectures and sizes.

E ADDITIONAL ANALYSIS

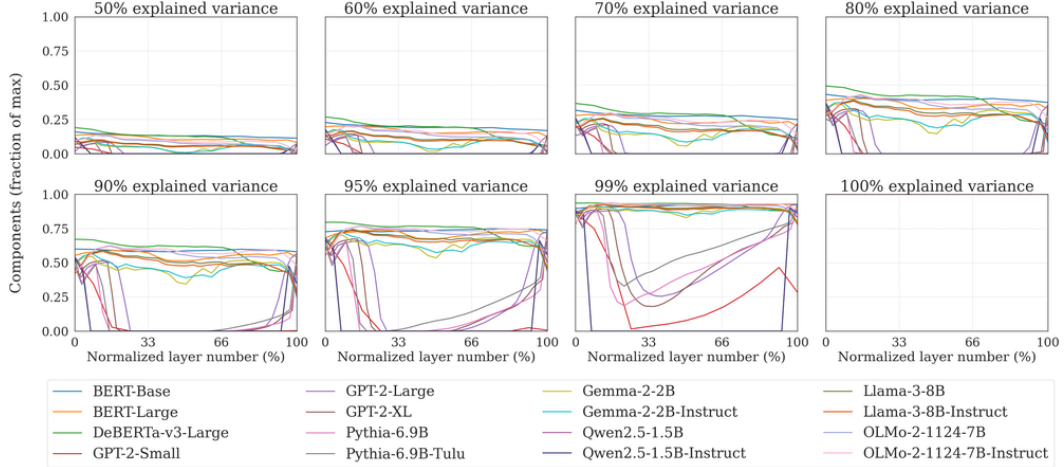


Figure 11: Intrinsic dimensionality across layers. Lines show fraction of PCA components needed to reach variance thresholds (50–100%). Models with strong mid-layer compression (few components for high variance) align with the inflection-is-linear, lemma-is-nonlinear split. Full curves per model appear in Figure 12.

E.1 INTRINSIC DIMENSIONALITY RESULTS

Model	d_{model}	ID ₅₀			ID ₇₀			ID ₉₀		
		First	Mid	Final	First	Mid	Final	First	Mid	Final
BERT-Base	768	123	100	88	244	212	192	461	451	446
BERT-Large	1024	138	105	85	286	226	208	567	527	554
DeBERTa-v3-Large	1024	196	133	29	377	299	113	688	635	423
GPT-2-Small	768	37	1	1	152	1	1	402	1	3
GPT-2-Large	1280	24	1	95	172	1	284	583	1	726
GPT-2-XL	1600	113	1	118	340	1	356	838	1	914
Pythia-6.9B	4096	391	1	96	865	1	517	1952	1	1925
Pythia-6.9B-Tulu	4096	390	1	244	862	1	832	1949	1	2292
OLMo-2-7B	4096	404	310	41	833	896	299	1772	2279	1550
OLMo-2-7B-Instruct	4096	404	358	111	833	974	567	1772	2361	1964
Gemma-2-2B	2304	216	8	11	505	130	70	1129	794	611
Gemma-2-2B-Instruct	2304	222	22	8	520	198	57	1153	899	572
Qwen-2.5-1.5B	1536	184	1	9	399	1	50	835	1	452
Qwen-2.5-1.5B-Instruct	1536	184	1	11	394	1	70	820	1	533
Llama-3.1-8B	4096	373	240	35	789	727	187	1722	2051	1119
Llama-3.1-8B-Instruct	4096	372	215	31	788	664	181	1722	1957	1093

Table 2: Number of principal-component axes required to reach 50% (ID₅₀), 70% (ID₇₀) and 90% (ID₉₀) explained variance in the first, middle and last layers of each model.

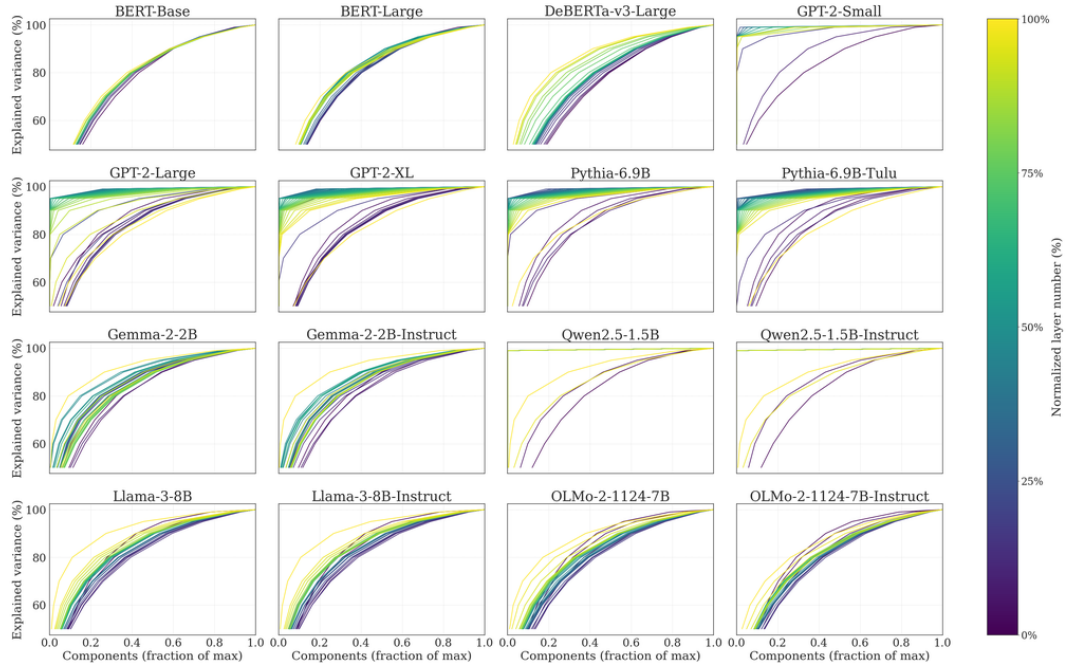


Figure 12: Intrinsic dimensionality curves for all models for English. Each subplot shows the relationship between the percentage of maximum PCA components (x-axis) and the percentage of explained variance (y-axis) across different layers. The color gradient from purple (early layers, 0%) to yellow (late layers, 100%) indicates the relative layer depth within each model. Models like BERT, Gemma, and Llama show similar compression patterns, while GPT-2 variants, Qwen and Pythia exhibit opposite trends in their middle layers.

F DATASET STATISTICS

This section provides statistics and visualizations for the datasets and models used in our experiments across all six languages. Only words containing alphabetic characters and apostrophes were considered.

Language	Total Words	Unique Lemmas	Unique Forms	Inflection Types	Sentences	Avg. Length
English	54,816	7,848	11,720	8	8,415	6.5
Chinese	44,166	11,184	11,237	4	7,892	5.8
German	84,710	24,140	31,890	9	9,234	7.3
French	115,847	13,804	24,485	6	8,765	6.6
Russian	193,320	20,943	59,830	8	10,234	7.1
Turkish	20,881	3,776	11,680	7	6,789	6.4

Table 3: Dataset statistics across all six languages. Russian has the largest dataset and the highest number of unique forms, reflecting its rich inflectional morphology. Turkish has the fewest total words and lemmas, while Chinese has the fewest inflection types.

F.1 ENGLISH DATASET DETAILS

For the English GUM corpus specifically, the data covers three main syntactic categories: nouns (49.5%), verbs (31.2%), and adjectives (19.4%).

Table 4a shows the distribution of word categories in the English dataset, and Table 4b presents the distribution of inflection categories.

		Count	Percentage		
Singular	19830	36.2%			
Base	10076	18.4%			
Positive	9926	18.1%			
Plural	7281	13.3%			
		Count	Percentage		
Noun	27111	49.5		3rd Person	1413
Verb	17093	31.2		Comparative	403
Adjective	10612	19.4		Superlative	283

(a) Distribution of word categories

(b) Distribution of inflection categories

(c) Sentence length statistics

Table 4: Distribution statistics for the English dataset

F.2 TOKENIZATION STATISTICS

Model	Tokenizer Type
BERT Base/Large	WordPiece
DeBERTa V3 Large	SentencePiece
GPT-2 variants	BPE
Pythia variants	BPE
OLMo 2 variants	BPE (tiktoken)
Gemma 2 variants	SentencePiece
Qwen 2.5 variants	Byte-level BPE
Llama 3.1 variants	BPE (tiktoken)

Table 5: Tokenization strategies used by different model families. BPE means byte-pair encoding.

An important consideration for our analysis is how different models tokenize the words in our dataset. Table 6 shows tokenization statistics across the models we analyze. Encoder-only models like BERT and DeBERTa tend to split words into more tokens than decoder-only models like GPT-2 and Qwen2, which may affect how information is encoded across layers.

Model	Avg. tokens per word	Med. tokens per word	Max tokens per word	Percent multitoken
BERT variants	1.11	1.0	6.0	6.95
DeBERTa-v3-large	1.03	1.0	4.0	2.2
GPT-2 variants	1.52	1.0	5.0	42.25
Pythia-6.9B variants	1.48	1.0	5.0	39.1
OLMo2-7B variants	1.43	1.0	4.0	35.9
Gemma2-2B variants	1.19	1.0	4.0	16.55
Qwen2.5-1.5B variants	1.43	1.0	4.0	35.9
Llama-3.1-8B variants	1.43	1.0	4.0	35.85

Table 6: Tokenization statistics across different models (English only). Most models have an average of 1.0-1.5 tokens per word and a median of 1, indicating that most words are tokenized as a single unit. However, there is variation in the proportion of words split into multiple tokens. Decoder-only models (e.g., GPT-2, Pythia, Qwen2, LLaMA) split 35-42% of words, while BERT and DeBERTa variants split fewer words (2-7%). Maximum tokens per word range from 4 to 6 across all models.

F.3 EFFECTS OF TOKENIZATION

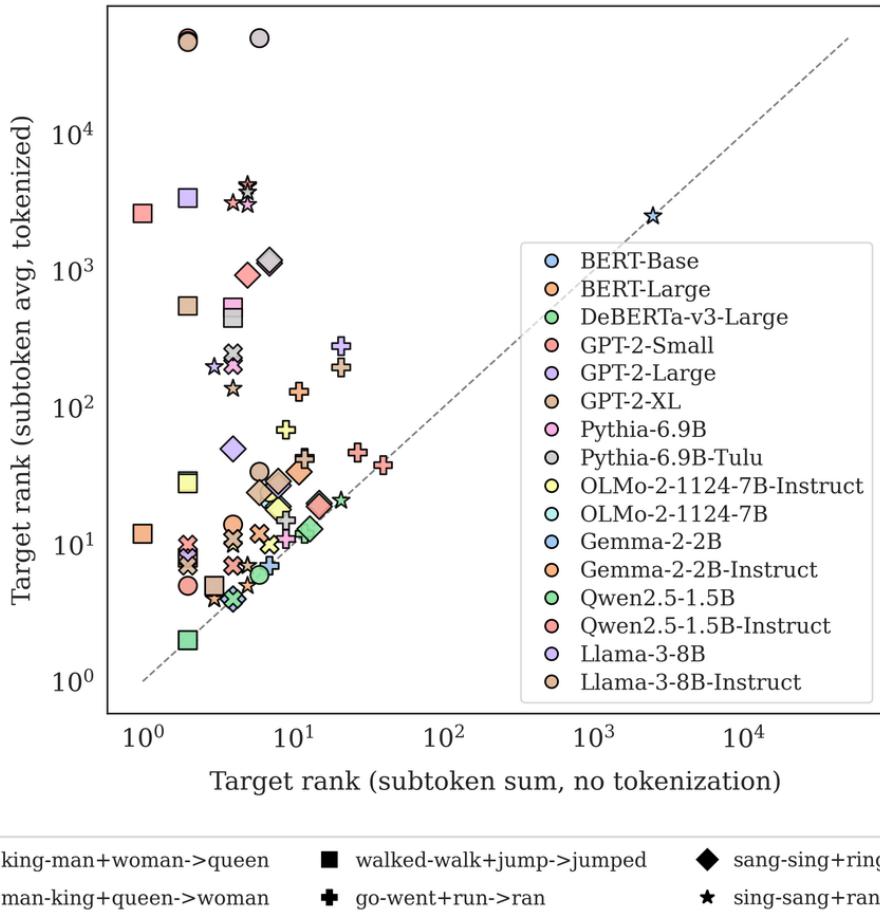


Figure 13: Effect of tokenization strategy on analogy completion rank. Each point corresponds to a model (color) and analogy (shape). The x-axis is the rank using whole-word representations. The y-axis is the rank using tokenized representations. Here, rank means the position of the expected word when all vocabulary words are sorted by similarity to the resulting embedding from vector arithmetic; lower is better. Points above the gray $y=x$ line mean tokenization hurts performance.

Tokenization is an essential component of language modeling. To test how tokenization influences our findings, we use analogy completion tasks in English (*e.g.*, *man:king::woman:?*) and compare two approaches: averaging subtoken embeddings after standard tokenization and summing embeddings from whole-word tokens.

For each approach, we perform vector arithmetic on word representations (*e.g.*, *king - man + woman*). We measure performance by ranking all vocabulary words by cosine similarity to the resulting representation, and observe how highly the expected word (*e.g.*, *queen*) ranks, with a lower rank indicating better performance.

Whole-word representations markedly outperform averaged subtokens across all models (Figure 13), implying that linguistic regularities are primarily stored in whole-word embeddings rather than compositionally across subtokens. Despite tokenization effects, our classifier results show consistent patterns across models using different tokenizers (see Table 5), indicating robust encoding of lexical and morphological information.

Model	HuggingFace ID
BERT-Base	bert-base-uncased
BERT-Large	bert-large-uncased
DeBERTa-v3-Large	microsoft/deberta-v3-large
mT5-base	google/mt5-base
GPT-2-Small	openai-community/gpt2
GPT-2-Large	openai-community/gpt2-large
GPT-2-XL	openai-community/gpt2-xl
Pythia-6.9B	EleutherAI/pythia-6.9b
Pythia-6.9B-Tulu	allenai/open-instruct-pythia-6.9b-tulu
OLMo-2-1124-7B	allenai/OLMo-2-1124-7B
OLMo-2-1124-7B-Instruct	allenai/OLMo-2-1124-7B-Instruct
Gemma-2-2B	google/gemma-2-2b
Gemma-2-2B-Instruct	google/gemma-2-2b-it
Qwen2.5-1.5B	Qwen/Qwen2.5-1.5B
Qwen2.5-1.5B-Instruct	Qwen/Qwen2.5-1.5B-Instruct
Qwen2.5-7B	Qwen/Qwen2.5-7B
Qwen2.5-7B-Instruct	Qwen/Qwen2.5-7B-Instruct
Llama-3.1-8B	meta-llama/Llama-3.1-8B
Llama-3.1-8B-Instruct	meta-llama/Llama-3.1-8B-Instruct
Goldfish English	goldfish-models/goldfish_eng_latn_1000mb
Goldfish Chinese	goldfish-models/goldfish_zho_hans_1000mb
Goldfish German	goldfish-models/goldfish_deu_latn_1000mb
Goldfish French	goldfish-models/goldfish_fra_latn_1000mb
Goldfish Russian	goldfish-models/goldfish_rus_cyr1_1000mb
Goldfish Turkish	goldfish-models/goldfish_tur_latn_1000mb

Table 7: Canonical HuggingFace model IDs used to load models in our study.

G ATTENTION HEAD ANALYSIS

We conducted additional experiments analyzing attention head outputs alongside residual stream representations to understand how different components of transformer models contribute to linguistic encoding.

G.1 METHODOLOGY

We averaged activations across all attention heads at each layer for Qwen2.5-1.5B and Qwen2.5-1.5B-Instruct models using the English dataset. We then trained linear regression, MLP, and random forest classifiers on both attention head outputs and residual stream representations to compare their encoding patterns.

G.2 RESULTS

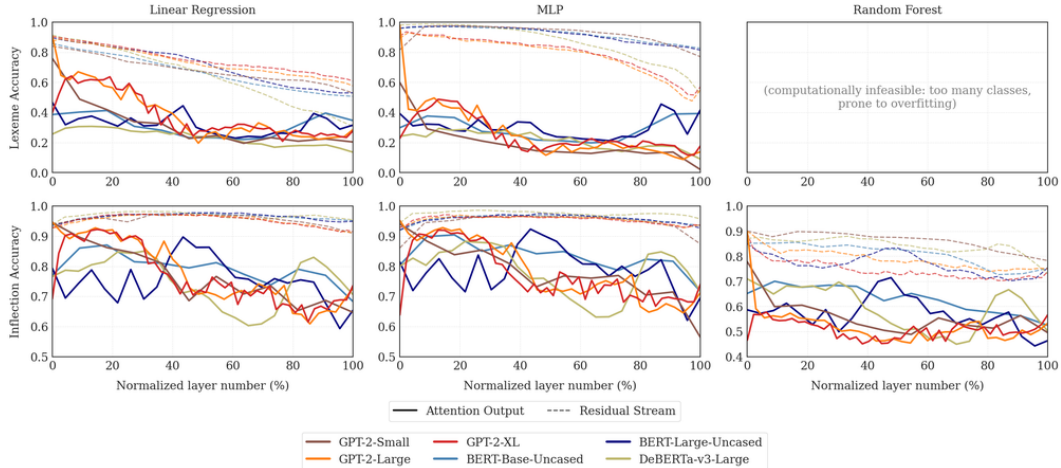


Figure 14: Linguistic task accuracy for attention head outputs (solid lines) versus residual stream representations (dashed lines) across BERT and GPT-2 model families. Top row shows lemma accuracy, bottom row shows inflection accuracy. Columns represent different classifier types. Attention outputs show pronounced drops in lexical accuracy during middle layers, while residual streams maintain higher performance. Both streams maintain high inflectional accuracy, though residual streams consistently outperform attention outputs.

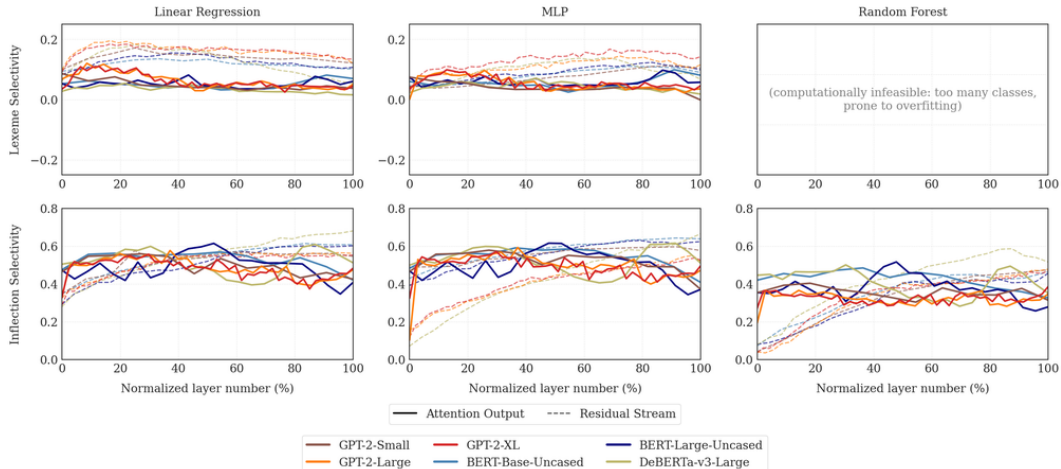


Figure 15: Classifier selectivity for attention head outputs (solid lines) versus residual stream representations (dashed lines) across BERT and GPT-2 model families. Top row shows lemma selectivity, bottom row shows inflection selectivity. Attention outputs show near-zero lemma selectivity throughout all layers, while inflection selectivity reaches moderate levels (0.4-0.5) in both streams, with residual streams showing slightly higher values.

The attention analysis reveals distinct encoding patterns between attention heads and residual streams. For lexical information, residual streams maintain relatively high accuracy (0.6-0.9) with gradual decline, while attention outputs show sharp drops to 0.2-0.4 in middle layers before modest recovery. For inflectional morphology, both components maintain high accuracy (0.7-1.0), though residual streams consistently outperform attention outputs, particularly in middle layers.

Selectivity analysis confirms that attention heads encode inflectional information more than lexical information, with inflection selectivity reaching 0.4-0.5 while lemma selectivity remains near zero. This supports the hypothesis that attention mechanisms primarily handle contextual relationships rather than parametric lexical knowledge.

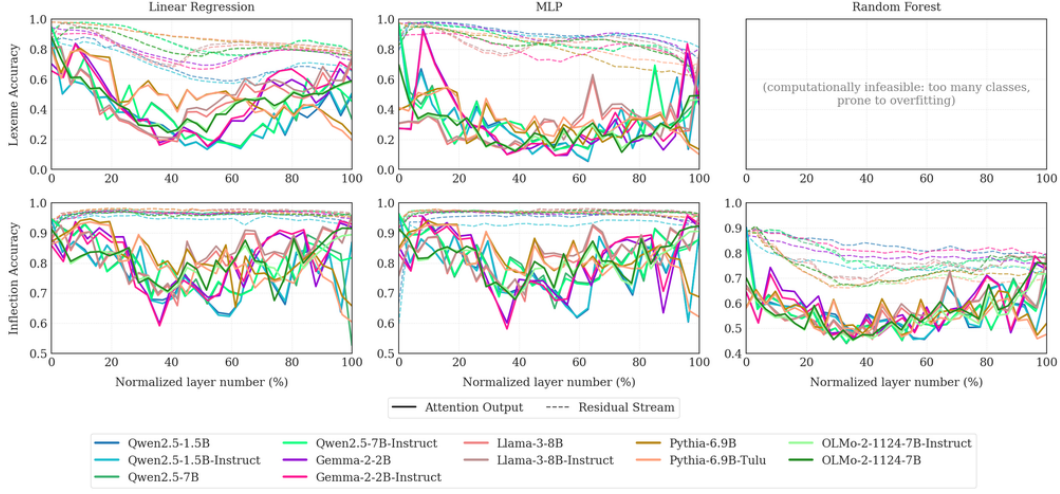


Figure 16: Linguistic task accuracy for attention head outputs (solid lines) versus residual stream representations (dashed lines) across contemporary model families. Top row shows lemma accuracy, bottom row shows inflection accuracy. The pattern of attention outputs showing lower lexical accuracy in middle layers is consistent across all model families, while inflectional accuracy remains high in both streams.

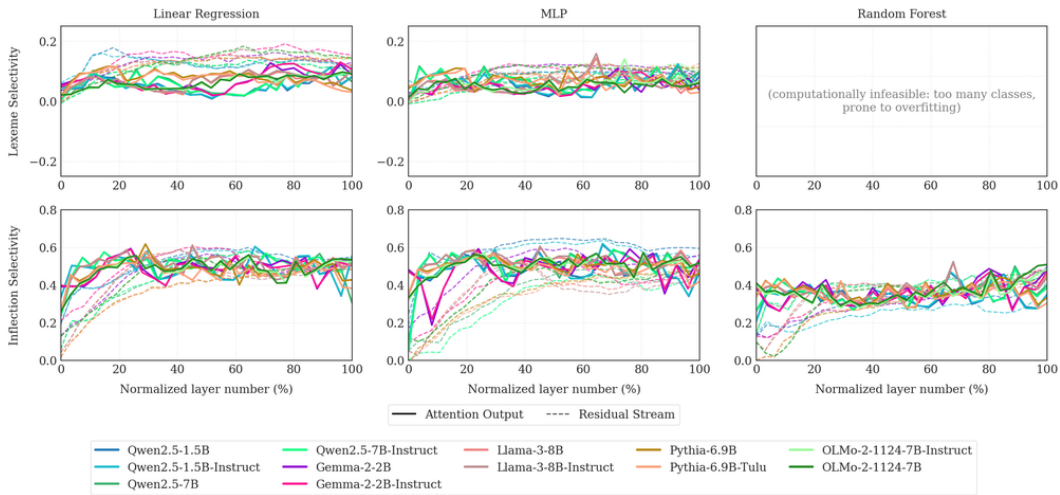


Figure 17: Classifier selectivity for attention head outputs (solid lines) versus residual stream representations (dashed lines) across contemporary model families. The selectivity patterns mirror those seen in BERT and GPT-2 families, with attention outputs maintaining near-zero lemma selectivity and moderate inflection selectivity across all models.

H STEERING VECTOR ANALYSIS

We conducted steering vector experiments to test whether inflectional representations can be functionally manipulated and to understand model sensitivity to activation interventions.

H.1 METHODOLOGY

For each inflectional category, we computed steering vectors as:

$$\mathbf{s}_i = \mu_i - \lambda \cdot \frac{1}{|C| - 1} \sum_{j \in C, j \neq i} \mu_j \quad (8)$$

We tested multiple values of λ (1, 5, 10, 20, 100) and measured the impact on MLP classifier performance when adding these steering vectors to existing activations for 1000 test words. We evaluated both mean probability change and prediction flip rate across all models.

H.2 RESULTS

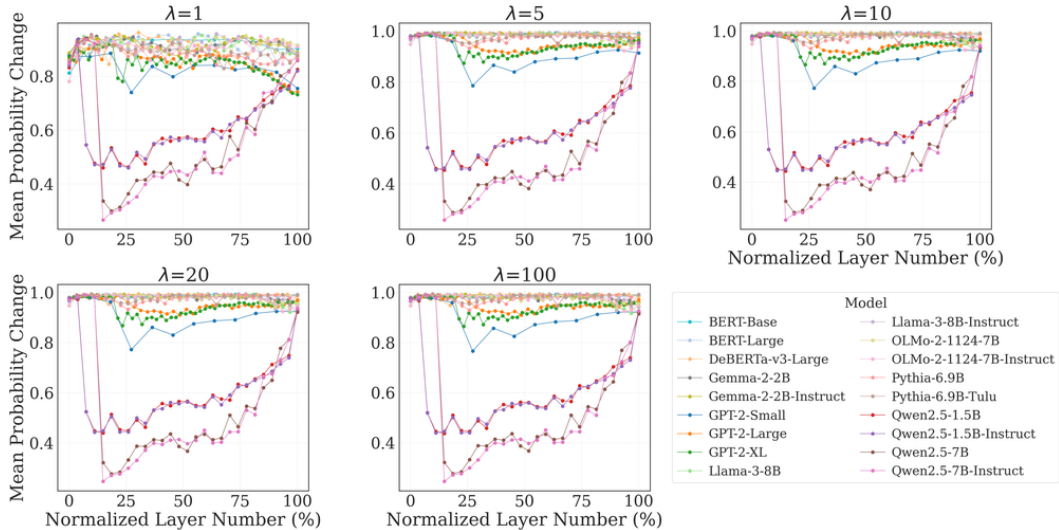


Figure 18: Mean probability change for inflection prediction when applying steering vectors across different λ values. Five panels show results for $\lambda \in \{1, 5, 10, 20, 100\}$. All models start with high effectiveness ($\approx 0.9-1.0$) at layer 0. Most models maintain stable performance, but Qwen2.5 variants show pronounced sensitivity dips around 10% layer depth before recovering. Higher λ values increase steering effectiveness while preserving the overall pattern.

Steering vector analysis demonstrates that inflectional representations can be effectively manipulated across most models and layers. The majority of models show robust steering effectiveness (>0.95 mean probability change and flip rate) throughout all layers, indicating that inflectional information is functionally accessible and modifiable.

However, we observe model-specific sensitivity patterns. The Qwen2.5 variants show pronounced vulnerability in middle layers (around 10% depth), where steering effectiveness drops to 0.6-0.7 before recovering in later layers. This sensitivity pattern aligns with our intrinsic dimensionality findings, where these same models show extreme compression in middle layers (requiring only 1 component for 50-99% variance).

The consistency of steering effectiveness across different λ values suggests that the underlying representational structure, rather than intervention magnitude, determines steering success. This supports our conclusion that models with compressed middle-layer representations are more susceptible to activation interventions.

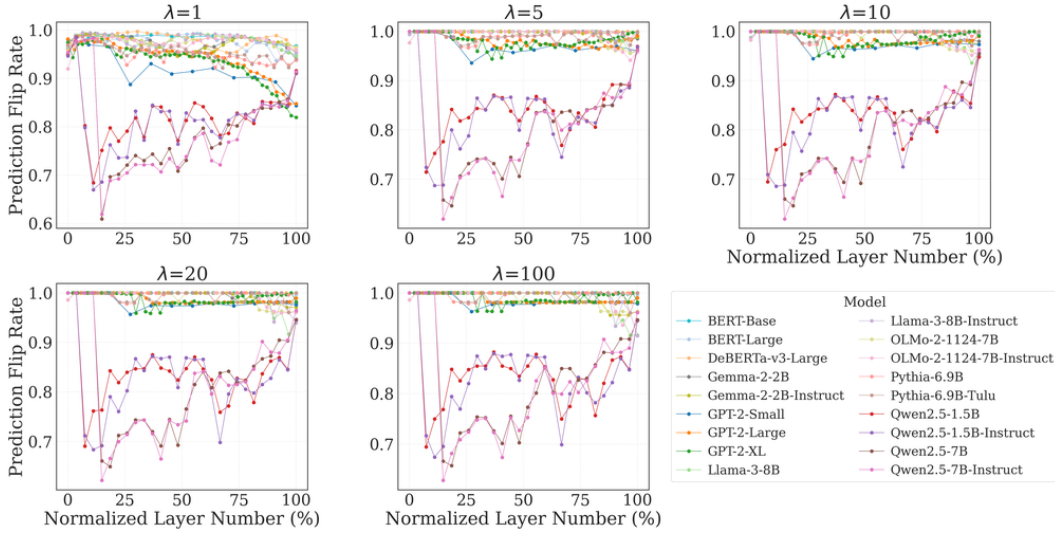


Figure 19: Prediction flip rate when applying steering vectors across different λ values. The flip rate patterns mirror the probability change results, with most models maintaining high rates (0.98-1.00) throughout all layers. Qwen2.5 variants show characteristic V-shaped dips to $\approx 0.60-0.70$ around 10% layer depth. The consistency across λ values suggests that steering effectiveness depends more on model architecture than intervention strength.

I RANDOM FOREST ANALYSIS

For our in-depth analysis of lexical information and inflectional morphology, we evaluated Random Forest classifiers as an additional non-linear baseline to complement our linear regression and MLP analyses.

I.1 RANDOM FOREST CLASSIFIER

Random forests provide a complementary approach to linear models by handling complex feature interactions and decision boundaries. Unlike linear models that assume information is linearly separable, random forests combine an often large number of decision trees via model averaging to robustly identify patterns (Breiman, 2001).

Since our classification tasks involve a large number of classes (thousands of unique lemmas and multiple inflection categories), we use a one-vs-all approach. For each class j , we train a binary random forest classifier that distinguishes class j from all other classes. Each binary classifier outputs a probability score $s_j(x) \in [0, 1]$ representing the confidence that input x belongs to class j . The final prediction is assigned based on the maximum score across all classes:

$$\hat{y} = \operatorname{argmax}_{j \in \{1, 2, \dots, c\}} s_j(x) \quad (9)$$

where $s_j(x)$ is the probability that the trained binary classifier assigns to class j for the input x .⁵

I.2 ENGLISH RESULTS

Lexical Identity Random Forest classifiers for lemma prediction were not comprehensively evaluated due to computational constraints arising from thousands of unique lemma classes. The one-vs-all training approach required for multi-class classification with Random Forests becomes prohibitively expensive with such a large number of classes.

⁵We use scikit-learn’s implementation (Pedregosa et al., 2011) with the `predict_proba()` method to obtain probability scores.

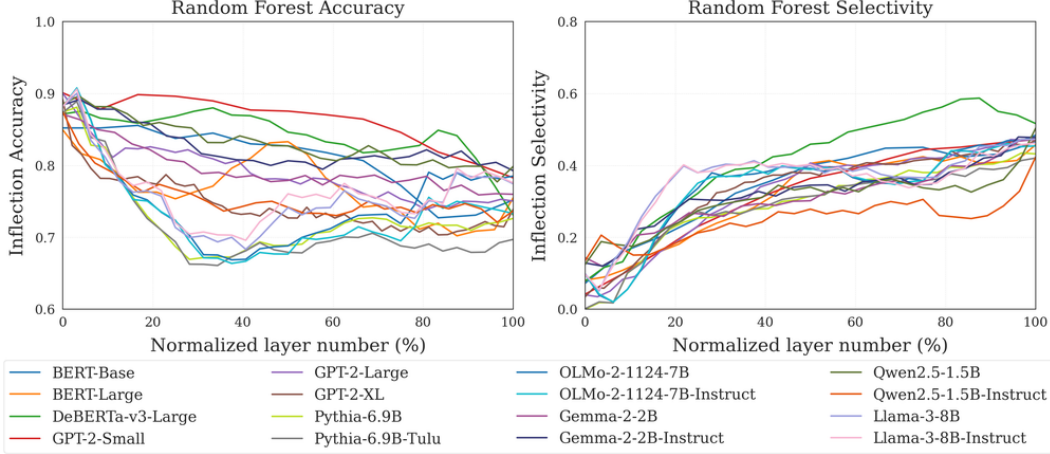


Figure 20: Random Forest classifier performance across model layers for English. The left column shows accuracy for lemma (top) and inflection (bottom) prediction. The right column shows classifier selectivity (difference between linguistic and control task accuracy) for the same tasks. Each line represents a different model.

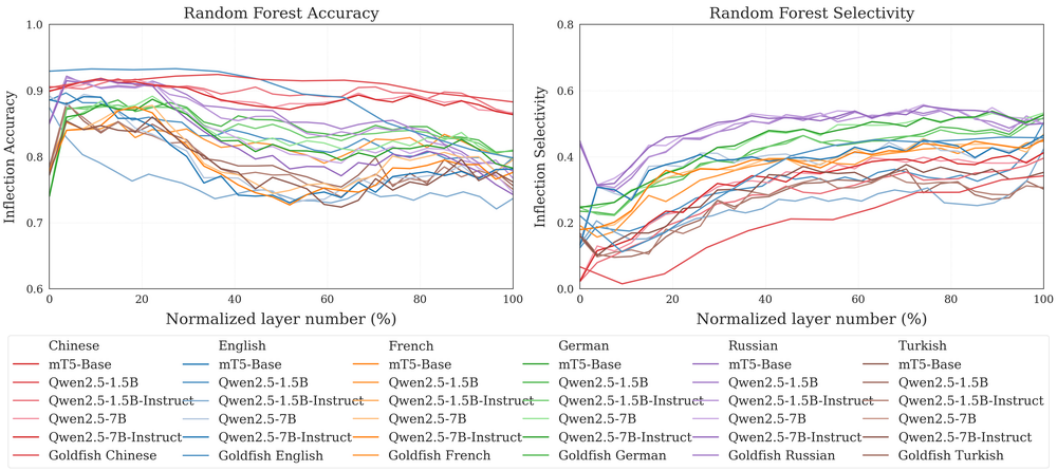


Figure 21: Random Forest classifier performance across languages and model layers. The left column shows accuracy for inflection prediction (lemma prediction omitted due to computational constraints with thousands of classes). The right column shows classifier selectivity.

Inflectional Morphology Random Forest classifiers for inflectional morphology show markedly different patterns compared to linear regression and MLP classifiers (Figure 20, bottom left). While linear and MLP classifiers maintain consistently high accuracy (0.9-1.0) across all layers, Random Forests exhibit lower overall accuracy (0.65-0.90) and a declining trend across layers. This contrasts sharply with the flat, high-performance curves observed for linear methods.

Selectivity Analysis Random Forest selectivity for inflectional morphology (Figure 20, bottom right) shows moderate values (0.2-0.4) but with more variability across models compared to linear methods. This suggests that while Random Forests can generalize beyond memorization, they are less consistent in their ability to extract the underlying morphological patterns compared to simpler linear approaches.

I.3 CROSS-LINGUISTIC PATTERNS

The multilingual Random Forest analysis (Figure 21) reveals consistent cross-linguistic patterns while highlighting language-specific challenges.

Cross-Linguistic Performance Random Forest classifiers for inflectional morphology show the same language ordering observed with linear and MLP classifiers: Russian and German achieve the highest accuracy (0.80-0.90), English and French show intermediate performance (0.70-0.85), Chinese maintains moderate accuracy (0.65-0.80), and Turkish consistently underperforms (0.55-0.75). This consistency across classifier types confirms that the observed patterns reflect genuine differences in how linguistic information is encoded rather than classifier-specific artifacts.

Selectivity Patterns Random Forest selectivity patterns are similar to those of linear classifiers but with greater variance. Russian and German maintain the highest selectivity (0.3-0.5), while Turkish shows the lowest (0.1-0.3). This consistency suggests that the underlying representational structure, rather than classifier choice, drives the observed cross-linguistic differences.

J CLASSIFIER ERROR ANALYSIS

We conducted a detailed error analysis of our classifiers to better understand their performance across different morphological features and languages. See Table 8 through Table 26 for the full results.

Model	3rd person (n=249)	Base (n=1,833)	Comparative (n=76)	Past (n=1,003)	Plural (n=1,247)	Positive (n=1,785)	Singular (n=3,587)	Superlative (n=52)
BERT-Base	0.960	0.965	0.817	0.967	0.983	0.946	0.971	0.759
BERT-Large	0.956	0.964	0.861	0.968	0.982	0.950	0.971	0.768
DeBERTa-v3-Large	0.938	0.974	0.831	0.961	0.986	0.954	0.977	0.706
GPT-2-Small	0.828	0.958	0.840	0.956	0.974	0.941	0.964	0.754
GPT-2-Large	0.812	0.958	0.826	0.951	0.975	0.936	0.967	0.792
GPT-2-XL	0.817	0.959	0.813	0.948	0.977	0.940	0.968	0.788
Pythia-6.9B	0.886	0.972	0.904	0.964	0.989	0.957	0.977	0.907
Pythia-6.9B-Tulu	0.899	0.973	0.909	0.967	0.989	0.956	0.976	0.910
OLMo-2-1124-7B	0.938	0.968	0.902	0.972	0.981	0.923	0.966	0.888
OLMo-2-1124-7B-Instruct	0.927	0.967	0.896	0.971	0.981	0.923	0.965	0.872
Gemma-2-2B	0.901	0.968	0.797	0.969	0.986	0.947	0.974	0.833
Gemma-2-2B-Instruct	0.913	0.966	0.863	0.973	0.988	0.938	0.972	0.872
Qwen2.5-1.5B	0.856	0.950	0.802	0.942	0.972	0.919	0.957	0.688
Qwen2.5-1.5B-Instruct	0.774	0.954	0.647	0.945	0.972	0.921	0.965	0.630

Table 8: Breakdown of inflection classification accuracy by morphological feature for each model using linear regression classifiers (English). Inflections are grouped by their morphological features (*e.g.*, Past, Plural, Comparative). For each group, the reported accuracy is the average of accuracies from classifiers trained at each model layer. All accuracy values are on a 0-1 scale. Comparative and superlative forms consistently show the lowest accuracy across all models, reflecting the challenges of these less frequent morphological categories.

Model	3rd person (n=249)	Base (n=1,833)	Comparative (n=76)	Past (n=1,003)	Plural (n=1,247)	Positive (n=1,785)	Singular (n=3,587)	Superlative (n=52)
BERT-Base	0.973	0.969	0.910	0.972	0.989	0.959	0.974	0.939
BERT-Large	0.967	0.970	0.910	0.973	0.988	0.961	0.975	0.931
DeBERTa-v3-Large	0.954	0.976	0.925	0.966	0.989	0.962	0.979	0.867
GPT-2-Small	0.921	0.963	0.928	0.952	0.972	0.930	0.963	0.870
GPT-2-Large	0.857	0.962	0.872	0.955	0.976	0.942	0.967	0.854
GPT-2-XL	0.921	0.963	0.928	0.952	0.972	0.930	0.963	0.870
Pythia-6.9B	0.932	0.972	0.921	0.961	0.982	0.949	0.971	0.886
Pythia-6.9B-Tulu	0.948	0.974	0.932	0.964	0.983	0.949	0.971	0.897
OLMo-2-1124-7B	0.957	0.968	0.926	0.966	0.989	0.949	0.973	0.905
OLMo-2-1124-7B-Instruct	0.939	0.967	0.903	0.967	0.988	0.949	0.973	0.873
Gemma-2-2B	0.913	0.967	0.863	0.968	0.990	0.950	0.976	0.907
Gemma-2-2B-Instruct	0.930	0.970	0.878	0.975	0.989	0.946	0.974	0.906
Qwen2.5-1.5B	0.882	0.948	0.822	0.943	0.974	0.927	0.957	0.736
Qwen2.5-1.5B-Instruct	0.808	0.953	0.697	0.947	0.974	0.930	0.965	0.682

Table 9: Breakdown of inflection classification accuracy by morphological feature for each model using MLP classifiers (English). Inflections are grouped by their morphological features (e.g., Past, Plural, Comparative). For each group, the reported accuracy is the average of accuracies from classifiers trained at each model layer. All accuracy values are on a 0–1 scale. MLP classifiers provide modest improvements over linear regression, particularly for comparative and superlative forms, though the relative ordering across morphological features remains consistent.

Model	Noun (n=1,739)	Verb (n=641)	Adjective (n=641)	Adverb (n=23)	Pronoun (n=1)	Preposition (n=1)	Conjunction (n=1)	Interjection (n=1)	Other (n=9)
BERT-Base	0.636	0.737	0.609	0.805	0.292	0.000	0.585	0.000	0.902
BERT-Large	0.684	0.777	0.653	0.826	0.580	0.154	0.662	0.065	0.897
DeBERTa-v3-Large	0.592	0.737	0.585	0.723	0.440	0.077	0.438	0.081	0.866
GPT-2-Small	0.631	0.789	0.612	0.813	0.542	0.000	0.415	0.033	0.896
GPT-2-Large	0.691	0.810	0.688	0.847	0.853	0.174	0.267	0.115	0.912
GPT-2-XL	0.713	0.827	0.708	0.847	0.724	0.222	0.311	0.241	0.899
Pythia-6.9B	0.856	0.926	0.836	0.926	0.938	0.443	0.566	0.488	0.934
Pythia-6.9B-Tulu	0.864	0.930	0.843	0.930	0.923	0.514	0.651	0.476	0.936
OLMo-2-1124-7B	0.798	0.875	0.794	0.913	0.697	0.339	0.363	0.495	0.913
OLMo-2-1124-7B-Instruct	0.798	0.868	0.792	0.902	0.606	0.339	0.331	0.495	0.910
Gemma-2-2B	0.757	0.869	0.736	0.876	0.667	0.179	0.205	0.288	0.891
Gemma-2-2B-Instruct	0.749	0.844	0.742	0.872	0.620	0.137	0.152	0.247	0.912
Qwen2.5-1.5B	0.652	0.801	0.650	0.828	0.526	0.082	0.223	0.068	0.867
Qwen2.5-1.5B-Instruct	0.642	0.800	0.632	0.831	0.544	0.082	0.245	0.068	0.877
Llama-3.1-8B	0.776	0.882	0.771	0.887	0.831	0.286	0.396	0.321	0.911
Llama-3.1-8B-Instruct	0.796	0.892	0.788	0.896	0.908	0.300	0.443	0.357	0.917

Table 10: Breakdown of lemma classification accuracy by Part of Speech (POS) for each model using linear regression classifiers (English). Lemmas are grouped by their POS tags (e.g., Noun, Verb, Adjective). For each group, the reported accuracy is the average of accuracies from classifiers trained at each model layer. All accuracy values are on a 0–1 scale. Performance varies significantly with frequency: frequent categories like nouns and verbs achieve higher accuracy, while infrequent categories like pronouns and prepositions show lower performance due to limited training examples.

Model	Noun (n=1,739)	Verb (n=641)	Adjective (n=641)	Adverb (n=23)	Pronoun (n=1)	Preposition (n=1)	Conjunction (n=1)	Interjection (n=1)	Other (n=9)
BERT-Base	0.775	0.831	0.748	0.873	0.458	0.125	0.756	0.267	0.898
BERT-Large	0.813	0.863	0.785	0.884	0.540	0.231	0.725	0.323	0.897
DeBERTa-v3-Large	0.689	0.803	0.682	0.802	0.700	0.115	0.662	0.242	0.861
GPT-2-Small	0.678	0.792	0.665	0.765	0.042	0.000	0.610	0.000	0.830
GPT-2-Large	0.754	0.837	0.755	0.827	0.347	0.188	0.596	0.385	0.871
GPT-2-XL	0.774	0.844	0.771	0.827	0.561	0.232	0.561	0.431	0.860
Pythia-6.9B	0.774	0.856	0.768	0.862	0.554	0.229	0.528	0.310	0.868
Pythia-6.9B-Tulu	0.818	0.880	0.803	0.887	0.554	0.343	0.613	0.381	0.889
OLMo-2-1124-7B	0.818	0.877	0.828	0.896	0.727	0.290	0.734	0.505	0.885
OLMo-2-1124-7B-Instruct	0.822	0.874	0.829	0.897	0.667	0.306	0.750	0.473	0.886
Gemma-2-2B	0.763	0.860	0.763	0.881	0.574	0.125	0.443	0.182	0.880
Gemma-2-2B-Instruct	0.777	0.846	0.785	0.882	0.580	0.137	0.400	0.299	0.875
Qwen2.5-1.5B	0.747	0.838	0.742	0.811	0.228	0.131	0.628	0.164	0.857
Qwen2.5-1.5B-Instruct	0.749	0.840	0.738	0.818	0.211	0.098	0.564	0.123	0.860
Llama-3.1-8B	0.798	0.879	0.807	0.886	0.800	0.214	0.679	0.393	0.882
Llama-3.1-8B-Instruct	0.824	0.893	0.826	0.895	0.831	0.257	0.689	0.429	0.887

Table 11: Breakdown of lemma classification accuracy by Part of Speech (POS) for each model using Multi-Layer Perceptron (MLP) classifiers (English). Lemmas are grouped by their POS tags (e.g., Noun, Verb, Adjective). For each group, the reported accuracy is the average of accuracies from classifiers trained at each model layer. All accuracy values are on a 0–1 scale. MLP classifiers provide consistent improvements over linear regression across all POS categories, though the frequency-dependent performance patterns persist.

Model	Linear Regression				MLP			
	Positive (n=300)	Base (n=2,074)	Plural (n=3)	Singular (n=3,947)	Positive (n=300)	Base (n=2,074)	Plural (n=3)	Singular (n=3,947)
mT5-Base	0.739	0.913	0.436	0.962	0.783	0.919	0.231	0.961
Qwen2.5-1.5B	0.785	0.929	0.034	0.969	0.801	0.924	0.092	0.967
Qwen2.5-1.5B-Instruct	0.779	0.925	0.034	0.964	0.803	0.923	0.057	0.967
Qwen2.5-7B	0.824	0.937	0.310	0.970	0.828	0.929	0.310	0.969
Qwen2.5-7B-Instruct	0.819	0.936	0.299	0.970	0.823	0.928	0.276	0.969
Goldfish Chinese	0.793	0.912	0.000	0.958	0.816	0.915	0.000	0.957

Table 12: Breakdown of inflection classification accuracy for each model by inflection type using Linear Regression and Multi-Layer Perceptron (MLP) classifiers (Chinese). Accuracies are calculated over all examples for a given group across all layers. Counts (n) are derived from a single representative layer for each group. All accuracy values are on a 0–1 scale.

Model	Noun (n=1,179)	Verb (n=564)	Adjective (n=108)	Adverb (n=22)	Preposition (n=20)	Other (n=50)
mT5-Base	0.838	0.828	0.786	0.762	0.920	0.726
Qwen2.5-1.5B	0.810	0.797	0.746	0.715	0.872	0.699
Qwen2.5-1.5B-Instruct	0.813	0.799	0.748	0.713	0.873	0.700
Qwen2.5-7B	0.887	0.882	0.846	0.847	0.915	0.817
Qwen2.5-7B-Instruct	0.886	0.877	0.843	0.835	0.913	0.811
Goldfish Chinese	0.883	0.878	0.845	0.875	0.954	0.858

Table 13: Breakdown of lemma classification accuracy by Part of Speech (POS) for each model, using Linear Regression classifiers (Chinese). Lemmas are grouped by their POS tags (e.g., Noun, Verb, Adjective). Accuracies are calculated over all examples for a given group across all layers. Counts (n) are derived from a single representative layer for each group. All accuracy values are on a 0–1 scale.

Model	Noun (n=1,179)	Verb (n=564)	Adjective (n=108)	Adverb (n=22)	Preposition (n=20)	Other (n=50)
mT5-Base	0.698	0.712	0.564	0.571	0.884	0.569
Qwen2.5-1.5B	0.748	0.761	0.658	0.668	0.826	0.669
Qwen2.5-1.5B-Instruct	0.735	0.745	0.643	0.643	0.814	0.655
Qwen2.5-7B	0.815	0.826	0.749	0.745	0.848	0.750
Qwen2.5-7B-Instruct	0.815	0.822	0.747	0.734	0.845	0.744
Goldfish Chinese	0.766	0.771	0.647	0.621	0.912	0.682

Table 14: Breakdown of lemma classification accuracy by Part of Speech (POS) for each model, using Multi-Layer Perceptron (MLP) classifiers (Chinese). Lemmas are grouped by their POS tags (*e.g.*, Noun, Verb, Adjective). Accuracies are calculated over all examples for a given group across all layers. Counts (n) are derived from a single representative layer for each group. All accuracy values are on a 0–1 scale.

Model	Base (n=417)	3rd person (n=517)	Positive (n=1,720)	Past (n=839)	Plural (n=1,076)	Superlative (n=52)	Singular (n=3,197)	Comparative (n=141)
mT5-Base	0.908	0.941	0.940	0.960	0.882	0.572	0.962	0.636
Qwen2.5-1.5B	0.849	0.889	0.922	0.914	0.888	0.657	0.953	0.796
Qwen2.5-1.5B-Instruct	0.844	0.887	0.922	0.910	0.889	0.659	0.952	0.795
Qwen2.5-7B	0.892	0.922	0.939	0.947	0.909	0.826	0.962	0.878
Qwen2.5-7B-Instruct	0.915	0.934	0.945	0.962	0.924	0.866	0.968	0.909
Goldfish German	0.938	0.941	0.955	0.979	0.916	0.542	0.968	0.708

Table 15: Breakdown of inflection classification accuracy for each model by inflection type using Linear Regression classifiers (German). Accuracies are calculated over all examples for a given group across all layers. Counts (n) are derived from a single representative layer for each group. All accuracy values are on a 0–1 scale.

Model	Base (n=417)	3rd person (n=517)	Positive (n=1,720)	Past (n=839)	Plural (n=1,076)	Superlative (n=52)	Singular (n=3,197)	Comparative (n=141)
mT5-Base	0.921	0.945	0.948	0.959	0.884	0.723	0.967	0.770
Qwen2.5-1.5B	0.890	0.915	0.930	0.940	0.897	0.831	0.958	0.892
Qwen2.5-1.5B-Instruct	0.888	0.914	0.930	0.938	0.898	0.825	0.957	0.897
Qwen2.5-7B	0.912	0.932	0.944	0.956	0.913	0.868	0.964	0.924
Qwen2.5-7B-Instruct	0.925	0.941	0.950	0.966	0.928	0.901	0.970	0.936
Goldfish German	0.947	0.957	0.964	0.978	0.923	0.817	0.970	0.896

Table 16: Breakdown of inflection classification accuracy for each model by inflection type using Multi-Layer Perceptron (MLP) classifiers (German). Accuracies are calculated over all examples for a given group across all layers. Counts (n) are derived from a single representative layer for each group. All accuracy values are on a 0–1 scale.

Model	Linear Regression				MLP			
	Noun (n=1,262)	Verb (n=395)	Adjective (n=406)	Other (n=12)	Noun (n=1,262)	Verb (n=395)	Adjective (n=406)	Other (n=12)
mT5-Base	0.685	0.662	0.568	0.750	0.611	0.602	0.486	0.723
Qwen2.5-1.5B	0.743	0.725	0.715	0.775	0.721	0.700	0.687	0.711
Qwen2.5-1.5B-Instruct	0.740	0.722	0.715	0.766	0.722	0.698	0.687	0.704
Qwen2.5-7B	0.821	0.809	0.808	0.829	0.795	0.786	0.783	0.814
Qwen2.5-7B-Instruct	0.815	0.803	0.803	0.821	0.795	0.785	0.782	0.813
Goldfish German	0.720	0.747	0.701	0.769	0.758	0.772	0.742	0.769

Table 17: Breakdown of lemma classification accuracy by Part of Speech (POS) for each model, using Linear Regression and Multi-Layer Perceptron (MLP) classifiers (German). Lemmas are grouped by their POS tags (*e.g.*, , Noun, Verb, Adjective). Accuracies are calculated over all examples for a given group across all layers. Counts (n) are derived from a single representative layer for each group. All accuracy values are on a 0–1 scale.

Model	Base (n=688)	3rd person (n=776)	Positive (n=1,833)	Past (n=857)	Plural (n=1,457)	Singular (n=5,169)
mT5-Base	0.934	0.912	0.879	0.908	0.954	0.970
Qwen2.5-1.5B	0.933	0.858	0.896	0.903	0.958	0.967
Qwen2.5-1.5B-Instruct	0.930	0.852	0.893	0.898	0.958	0.966
Qwen2.5-7B	0.955	0.918	0.918	0.931	0.965	0.975
Qwen2.5-7B-Instruct	0.951	0.913	0.915	0.928	0.964	0.974
Goldfish French	0.942	0.955	0.937	0.930	0.968	0.976

Table 18: Breakdown of inflection classification accuracy for each model by inflection type using Linear Regression classifiers (French). Accuracies are calculated over all examples for a given group across all layers. Counts (n) are derived from a single representative layer for each group. All accuracy values are on a 0–1 scale.

Model	Base (n=688)	3rd person (n=776)	Positive (n=1,833)	Past (n=857)	Plural (n=1,457)	Singular (n=5,169)
mT5-Base	0.957	0.937	0.911	0.935	0.957	0.977
Qwen2.5-1.5B	0.954	0.905	0.914	0.925	0.965	0.968
Qwen2.5-1.5B-Instruct	0.954	0.902	0.911	0.924	0.965	0.968
Qwen2.5-7B	0.966	0.936	0.930	0.937	0.970	0.976
Qwen2.5-7B-Instruct	0.962	0.931	0.926	0.934	0.970	0.975
Goldfish French	0.974	0.967	0.945	0.942	0.973	0.979

Table 19: Breakdown of inflection classification accuracy for each model by inflection type using Multi-Layer Perceptron (MLP) classifiers (French). Accuracies are calculated over all examples for a given group across all layers. Counts (n) are derived from a single representative layer for each group. All accuracy values are on a 0–1 scale.

Model	Linear Regression				MLP			
	Noun (n=1,496)	Verb (n=406)	Adjective (n=358)	Other (n=15)	Noun (n=1,496)	Verb (n=406)	Adjective (n=358)	Other (n=15)
	0.708	0.577	0.605	0.799	0.755	0.560	0.636	0.820
Qwen2.5-1.5B	0.754	0.725	0.673	0.824	0.807	0.765	0.751	0.853
Qwen2.5-1.5B-Instruct	0.750	0.718	0.671	0.820	0.824	0.776	0.768	0.869
Qwen2.5-7B	0.840	0.814	0.764	0.869	0.856	0.825	0.794	0.884
Qwen2.5-7B-Instruct	0.833	0.805	0.758	0.860	0.851	0.818	0.792	0.883
Goldfish French	0.749	0.758	0.661	0.811	0.894	0.869	0.813	0.888

Table 20: Breakdown of lemma classification accuracy by Part of Speech (POS) for each model, using Linear Regression and Multi-Layer Perceptron (MLP) classifiers (French). Lemmas are grouped by their POS tags (e.g., Noun, Verb, Adjective). Accuracies are calculated over all examples for a given group across all layers. Counts (n) are derived from a single representative layer for each group. All accuracy values are on a 0–1 scale.

Model	Base (n=690)	3rd person (n=456)	Positive (n=1,192)	Past (n=455)	Plural (n=1,333)	Superlative (n=3)	Singular (n=3,316)	Comparative (n=23)
mT5-Base	0.930	0.978	0.975	0.957	0.877	0.000	0.977	0.799
Qwen2.5-1.5B	0.925	0.946	0.974	0.938	0.923	0.015	0.966	0.835
Qwen2.5-1.5B-Instruct	0.924	0.943	0.974	0.934	0.921	0.015	0.966	0.817
Qwen2.5-7B	0.949	0.966	0.979	0.958	0.948	0.094	0.977	0.872
Qwen2.5-7B-Instruct	0.951	0.974	0.980	0.970	0.948	0.080	0.980	0.918
Goldfish Russian	0.940	0.950	0.976	0.931	0.921	0.000	0.976	0.867

Table 21: Breakdown of inflection classification accuracy for each model by inflection type using Linear Regression classifiers (Russian). Accuracies are calculated over all examples for a given group across all layers. Counts (n) are derived from a single representative layer for each group. All accuracy values are on a 0–1 scale.

Model	Base (n=690)	3rd person (n=456)	Positive (n=1,192)	Past (n=455)	Plural (n=1,333)	Superlative (n=3)	Singular (n=3,316)	Comparative (n=23)
mT5-Base	0.959	0.978	0.969	0.966	0.904	0.000	0.978	0.849
Qwen2.5-1.5B	0.952	0.955	0.972	0.948	0.933	0.089	0.970	0.899
Qwen2.5-1.5B-Instruct	0.950	0.954	0.973	0.947	0.933	0.089	0.969	0.911
Qwen2.5-7B	0.963	0.964	0.978	0.960	0.951	0.246	0.979	0.910
Qwen2.5-7B-Instruct	0.961	0.970	0.978	0.966	0.949	0.126	0.980	0.924
Goldfish Russian	0.965	0.972	0.978	0.948	0.943	0.000	0.977	0.934

Table 22: Breakdown of inflection classification accuracy for each model by inflection type using Multi-Layer Perceptron (MLP) classifiers (Russian). Accuracies are calculated over all examples for a given group across all layers. Counts (n) are derived from a single representative layer for each group. All accuracy values are on a 0–1 scale.

Model	Linear Regression				MLP			
	Noun (n=982)	Verb (n=333)	Adjective (n=275)	Other (n=4)	Noun (n=982)	Verb (n=333)	Adjective (n=275)	Other (n=4)
	0.660	0.614	0.542	0.648	0.492	0.484	0.387	0.426
mT5-Base	0.660	0.614	0.542	0.648	0.492	0.484	0.387	0.426
Qwen2.5-1.5B	0.777	0.712	0.759	0.720	0.712	0.696	0.716	0.647
Qwen2.5-1.5B-Instruct	0.772	0.704	0.756	0.720	0.710	0.689	0.717	0.643
Qwen2.5-7B	0.854	0.790	0.843	0.812	0.798	0.794	0.813	0.749
Qwen2.5-7B-Instruct	0.845	0.778	0.835	0.807	0.794	0.785	0.809	0.744
Goldfish Russian	0.795	0.723	0.764	0.676	0.810	0.776	0.759	0.657

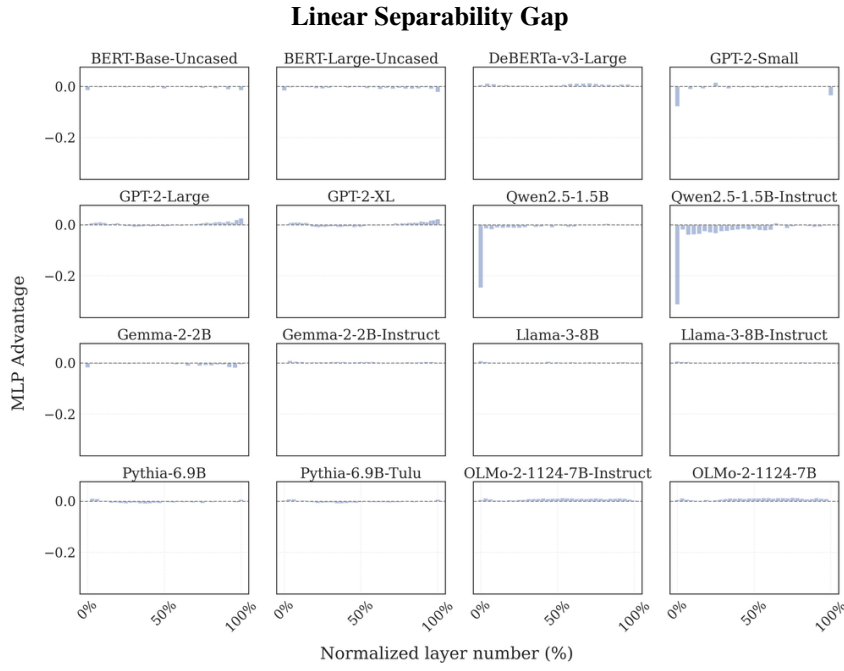
Table 23: Breakdown of lemma classification accuracy by Part of Speech (POS) for each model, using Linear Regression and Multi-Layer Perceptron (MLP) classifiers (Russian). Lemmas are grouped by their POS tags (*e.g.*, , Noun, Verb, Adjective). Accuracies are calculated over all examples for a given group across all layers. Counts (n) are derived from a single representative layer for each group. All accuracy values are on a 0–1 scale.

Model	Base (n=154)	3rd person (n=51)	Positive (n=401)	Past (n=168)	Plural (n=33)	Singular (n=632)
mT5-Base	0.860	0.911	0.928	0.966	0.837	0.952
Qwen2.5-1.5B	0.808	0.802	0.721	0.928	0.861	0.892
Qwen2.5-1.5B-Instruct	0.809	0.817	0.720	0.941	0.878	0.899
Qwen2.5-7B	0.865	0.879	0.810	0.966	0.903	0.909
Qwen2.5-7B-Instruct	0.850	0.874	0.796	0.960	0.886	0.900
Goldfish Turkish	0.847	0.915	0.880	0.964	0.872	0.963

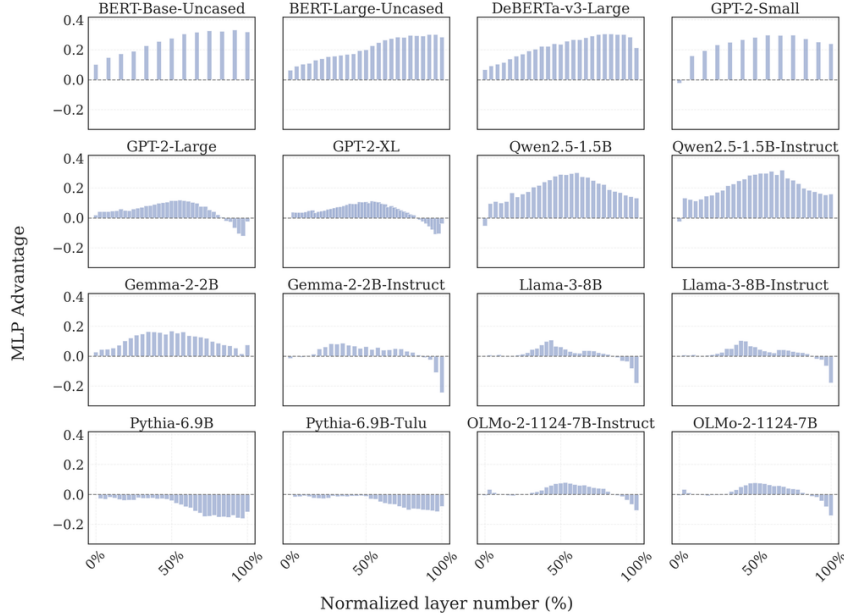
Table 24: Breakdown of inflection classification accuracy for each model by inflection type using Linear Regression classifiers (Turkish). Accuracies are calculated over all examples for a given group across all layers. Counts (n) are derived from a single representative layer for each group. All accuracy values are on a 0–1 scale.

Model	Base (n=154)	3rd person (n=51)	Positive (n=401)	Past (n=168)	Plural (n=33)	Singular (n=632)
mT5-Base	0.755	0.760	0.848	0.922	0.515	0.949
Qwen2.5-1.5B	0.770	0.767	0.667	0.919	0.765	0.914
Qwen2.5-1.5B-Instruct	0.762	0.757	0.662	0.917	0.766	0.913
Qwen2.5-7B	0.853	0.845	0.791	0.956	0.875	0.937
Qwen2.5-7B-Instruct	0.845	0.844	0.786	0.956	0.875	0.932
Goldfish Turkish	0.832	0.879	0.870	0.957	0.834	0.957

Table 25: Breakdown of inflection classification accuracy for each model by inflection type using Multi-Layer Perceptron (MLP) classifiers (Turkish). Accuracies are calculated over all examples for a given group across all layers. Counts (n) are derived from a single representative layer for each group. All accuracy values are on a 0–1 scale.



(a) Linear separability gap for inflection prediction



(b) Linear separability gap for lemma prediction

Figure 22: Performance advantage of MLP classifiers over linear classifiers (in percentage points) across model layers for English. The linear separability gap measures how much a non-linear transformation improves classifier performance compared to a simple linear mapping. For inflection prediction, the gap is consistently minimal (mostly within ± 0.02 percentage points) and sometimes negative, indicating that inflectional features are primarily encoded in a linear fashion throughout the network. By contrast, the linear separability gap for lemma prediction is relatively large (0.1–0.3 percentage points) and positive across most models

Cross-Linguistic Linear Separability Gap

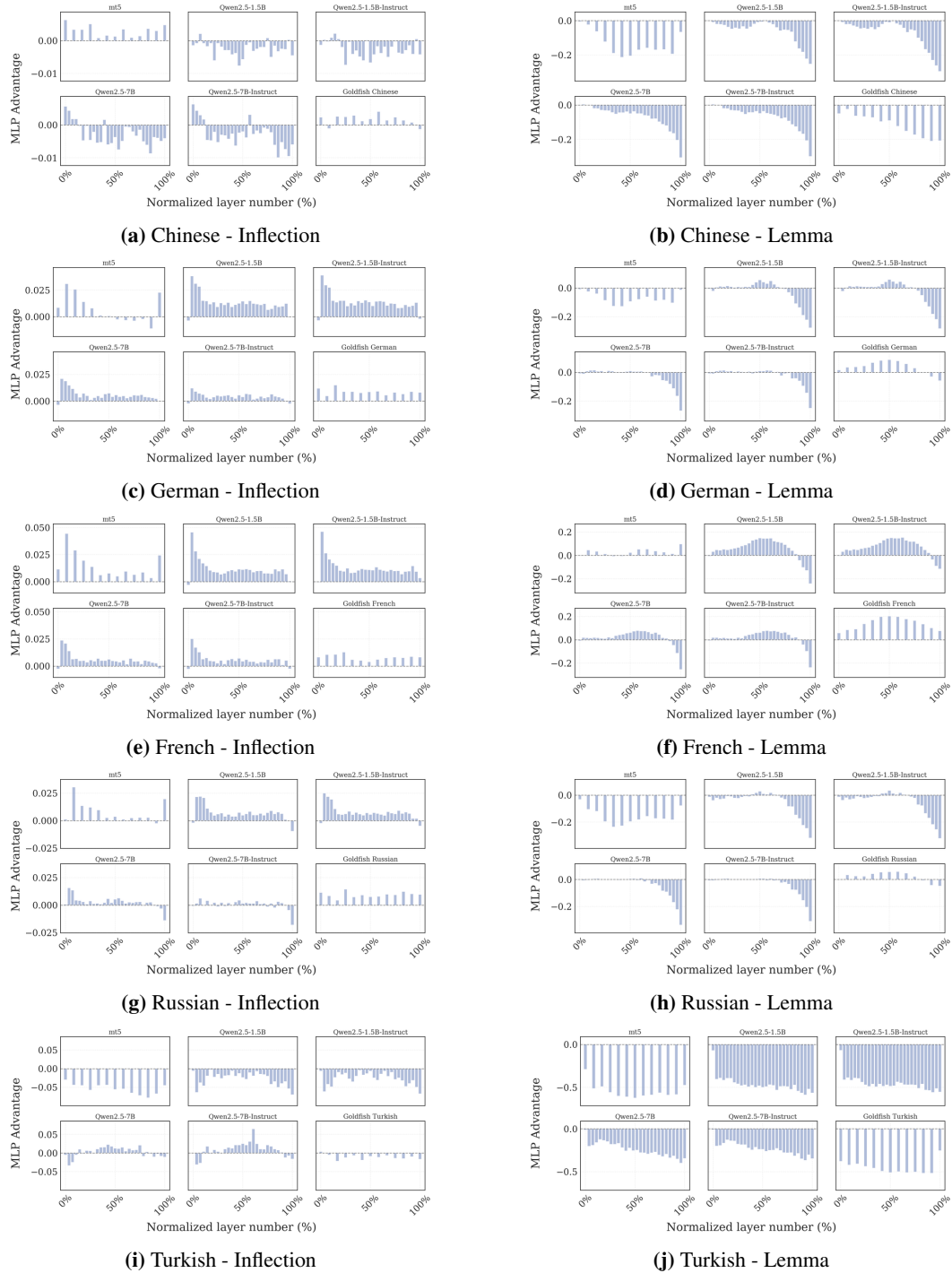


Figure 23: Cross-linguistic linear separability gap showing performance advantage of MLP classifiers over linear classifiers across model layers for five additional languages. For inflectional features, mT5 and Goldfish models show slight positive gaps (indicating modest benefits from non-linear classification), while Qwen2.5 variants show slight negative gaps (indicating linear classifiers are sufficient or superior). For lexical features, all models show negative gaps that are most pronounced in early layers, suggesting that linear regression with regularization consistently outperforms MLPs for lexical classification across all model families and languages.

Model	Linear Regression				MLP			
	Noun (n=221)	Verb (n=53)	Adjective (n=104)	Other (n=13)	Noun (n=221)	Verb (n=53)	Adjective (n=104)	Other (n=13)
	0.866	0.823	0.921	0.955	0.215	0.421	0.374	0.637
Qwen2.5-1.5B	0.834	0.805	0.866	0.877	0.307	0.439	0.449	0.693
Qwen2.5-1.5B-Instruct	0.816	0.791	0.860	0.874	0.305	0.439	0.448	0.691
Qwen2.5-7B	0.871	0.850	0.900	0.904	0.595	0.625	0.695	0.809
Qwen2.5-7B-Instruct	0.850	0.823	0.883	0.885	0.579	0.613	0.678	0.800
Goldfish Turkish	0.929	0.904	0.940	0.969	0.386	0.550	0.477	0.808

Table 26: Breakdown of lemma classification accuracy by Part of Speech (POS) for each model, using Linear Regression and Multi-Layer Perceptron (MLP) classifiers (Turkish). Lemmas are grouped by their POS tags (*e.g.*, , Noun, Verb, Adjective). Accuracies are calculated over all examples for a given group across all layers. Counts (n) are derived from a single representative layer for each group. All accuracy values are on a 0–1 scale.

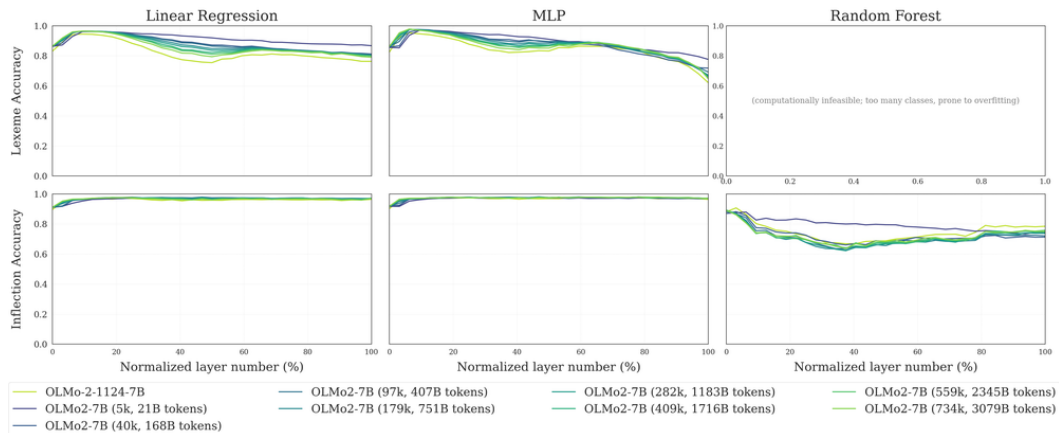


Figure 24: Lemma (top row) and inflection (bottom row) prediction accuracy across normalized layer number for OLMo-2-7B checkpoints at various pretraining steps (5k-734k steps) for English. The full model is 928k steps. Checkpoints are on a color gradient from brightest (earliest) to darkest (latest). Early checkpoints exhibit higher lemma accuracy than later ones, while inflectional accuracy remains flat across layers and checkpoints.

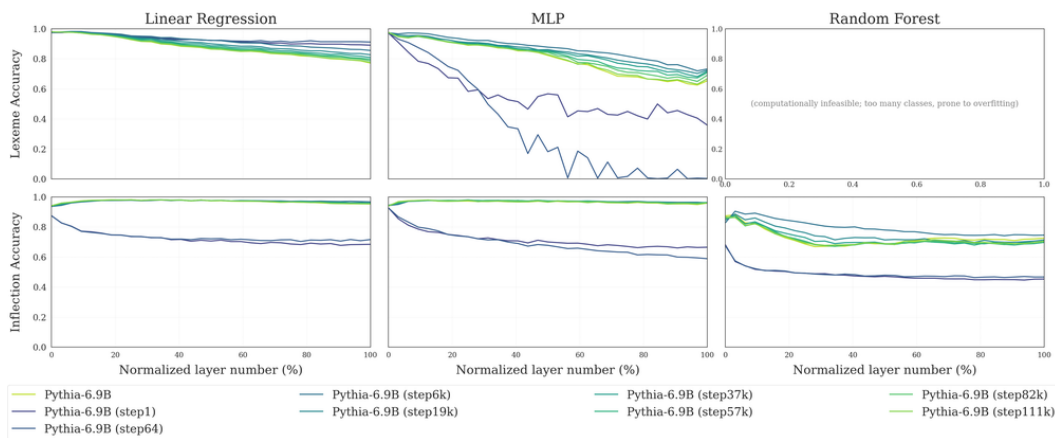


Figure 25: Lemma (top row) and inflection (bottom row) prediction accuracy across normalized layer number for Pythia-6.9B checkpoints at various pretraining steps (1-111k steps) for English. The full model is 143k steps. Checkpoints are on a color gradient from brightest (earliest) to darkest (latest). Lemma accuracy declines both with deeper layers and with more training, whereas inflectional accuracy stays uniformly high across all layers and checkpoints.